



Validation of Operational Multiscale Environment Model
With Grid Adaptivity (OMEGA)

THESIS

Gordon R. Taylor, Captain, USAF

AFIT/GEE/ENP/95D-10

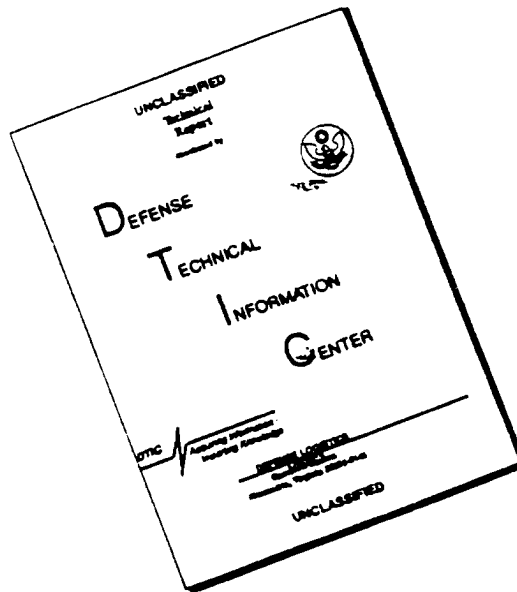
DISTRIBUTION STATEMENT H

Approved for public release
Distribution Unlimited

DEPARTMENT OF THE AIR FORCE
AIR UNIVERSITY
AIR FORCE INSTITUTE OF TECHNOLOGY

Wright-Patterson Air Force Base, Ohio

DISCLAIMER NOTICE



THIS DOCUMENT IS BEST QUALITY AVAILABLE. THE COPY FURNISHED TO DTIC CONTAINED A SIGNIFICANT NUMBER OF PAGES WHICH DO NOT REPRODUCE LEGIBLY.

AFIT/GEE/ENP/95D-10

Validation of Operational Multiscale Environment Model
With Grid Adaptivity (OMEGA)

THESIS

Gordon R. Taylor, Captain, USAF

AFIT/GEE/ENP/95D-10

Approved for public release; distribution unlimited

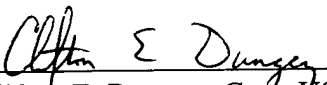
19960409 146

AFIT/GEE/ENP/95D-10

VALIDATION OF OPERATIONAL MULTISCALE ENVIRONMENT MODEL WITH
GRID ADAPTIVITY (OMEGA)

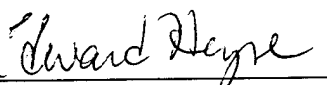
Gordon R. Taylor, B.S.
Captain, USAF

Approved:



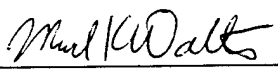
Clifton E. Dungey, Capt, USAF
Chairman

30 NOV 95
(date)



Edward C. Heyse, Maj, USAF

30 NOV 95
(date)



Michael K. Walters, Lt Col, USAF

30 NOV 95
(date)

The views expressed in the thesis are those of the author and do not reflect the official policy or position of the Department of Defense or the U.S. Government.

AFIT/GEE/ENP/95D-10

VALIDATION OF OPERATIONAL MULTISCALE ENVIRONMENT MODEL
WITH GRID ADAPTIVITY (OMEGA)

THESIS

Presented to the Faculty of the School of Engineering
of the Air Force Institute of Technology
Air University
In Partial Fulfillment of the
Requirements for the Degree of Master of Science

Gordon R. Taylor, B.S.

Captain, USAF

December 1995

Approved for public release; distribution unlimited

Acknowledgements

There are several persons I would like to thank for their help making this thesis possible. I thank my advisor, Cliff Dungey, for his great interest in this research and help coordinating with the Defense Nuclear Agency. Jim Hill, a contractor with DNA, opened up an account for me and tutored me through the model setup, providing countless times of running the model, downloading data, and making comparisons. Dr Sarma from Science Applications International Corporation provided test releases of the code still under development, and I thank him for his time and for including AFIT in SAIC's development process.

Support from others at AFIT proved invaluable. Charlie Brennan provided UNIX and FORTRAN knowledge indispensable to my efforts. AFIT/SC provided great service with their staff. Tim Schooler, Joe Hamlin, and David Dokes provided invaluable assistance.

Close to home, I thank my wife for her encouragement that started from the very first week--a honeymoon shortened so I could go TDY to Washington, D.C.

Most importantly, overreaching all the persons who assisted me, is my heavenly Father, and His Son Jesus Christ. "But my God shall supply all your need according to his riches in glory by Christ Jesus." Philippians 4:19.

Table of Contents

Acknowledgement	ii
List of Figures	v
Abstract	vi
1. Introduction	1
2. Literature Review	4
2.1 Introduction	4
2.2 Elements of Atmospheric Transport Models	7
2.3 Complications of Modelling	9
2.4 Example of Models	10
2.4.1 Newton Relaxation	11
2.4.2 Gaussian Plume Models	12
2.4.3 Air Resources Laboratories	14
2.4.4 Worldwide Version of System for Prediction of Environmental Emergency Dose Information	15
2.4.5 Canadian Tracer Model	16
2.4.6 Mass-adjusted, Three-dimensional Wind Field Model	20
2.4.7 MEDIA	21
2.4.8 Long Range Atmospheric Advection of Nuclides	22
2.5 Evaluation of Models	24
3. Methodology	27
3.1 Use of Medium Range Forecast Data over U.S.	27
3.2 Verification with High Resolution Analysis System Data and the Chernobyl Nuclear Accident	30
3.2.1 Background of HIRAS Data	30
3.2.2 Atmospheric Transport Model Evaluation Study Requirements	33
3.2.3 Methods Used for OMEGA	33
4. Results of OMEGA Validation	37
4.1 Medium Range Forecast Data Validation	39
4.2 High Resolution Analysis System Data Validation	44
4.3 Comment on Results	49
5. Conclusion	50
5.1 Achievement of Objectives	50
5.2 Recommendations	51

Appendix A: OMEGA Generated Grids for MRF and HIRAS Validation

Appendix B: Wind Field Tables for MRF and HIRAS Validation

Appendix C: National Weather Service Maps and OMEGA Generated Maps for
MRF Validation

Appendix D: Sample Maps for Deposition Using HIRAS Data

Appendix E: Chernobyl Source Term Defined by Fortran 90 Code

Bibliography

Vita

List of Figures

1. Gaussian Plume Distribution	13
2. Domain Over U.S. for MRF Data Run	31
3. Domain Over Europe for HIRAS Data Run	36
4. Error Plot of Wind Speeds for Dayton, OH	41
5. Error Plot of Wind Speeds for Pittsburgh, PA	42
6. Error Plot of Wind Speeds for Huntington, WV	43
7. Error Plot of Wind Speeds for Europe	45
8. Comparison of Deposition Maps for April 27, 1986	47
9. Comparison of Deposition Maps for April 28, 1986	48

Abstract

The Defense Nuclear Agency (DNA) is improving the military's capability to forecast dosage and hazard levels due to release of chemical, biological and nuclear agents. During Operation DESERT STORM the military realized the need for models to predict risk levels for military personnel assigned proximate to missile attacks. One project associated with this is the continuing development of the Operational Multiscale Environment Model with Grid Adaptivity (OMEGA). DNA has sponsored AFIT to validate OMEGA with focus on incorporating weather data obtained from Air Force Combat Climatology Center for the period of the Chernobyl Nuclear Accident. The physics of the model is tested using National Weather Service Medium Range Forecast data by comparing predicted wind fields for three weather stations with analysis maps. The model is further tested using the data generated at Air Force Global Weather Central for the first three days following the release at the Chernobyl Nuclear Plant. A user-defined source term was developed to simulate the release of radionuclides from the plant. Analysis from paired t-tests shows statistically how well OMEGA predicts wind fields. The results show qualitatively the promise of OMEGA to meet the needs of the Defense Nuclear Agency as the model is still under development.

Validation of Operational Multiscale Environment Model

With Grid Adaptivity (OMEGA)

1. Introduction

The Defense Nuclear Agency is interested in improving its capability to forecast dosage and hazard levels due to release of chemical, biological, or nuclear agents. Accidents of the magnitude of the Chernobyl Nuclear Accident, explosions like Mount Saint Helens, and the chemical spill in India show the need for forecast models to predict the transport of agents. During Operation DESERT STORM Scud missile attacks by Iraq provided such a challenge to the military. The ability to predict transport of these agents after release is vital to the survival of our military and therefore mission enhancing. During a crisis a model could be running continually with real or simulated sources. This would allow full modeling of conditions within the domain of interest before sources are introduced and produce better results.

Traditionally, atmospheric/mass transport models use rectangular grids or polar stereographs for terrain with coarse grid resolution. The OMEGA model grid is unstructured horizontally; it currently adapts to underlying surface features. The model has a variable horizontal grid resolution that can range from 1 km to 100 km and a vertical resolution ranging from a few meters to 1 km.

Advances in models resolve local perturbations on the larger scale wind field. These techniques require considering physical variables and processes affecting the flow,

such as topography, land use, land/water interfaces, vegetation, soil moisture, surface moisture, and energy budgets.

OMEGA uses a non-hydrostatic equation set to describe the dynamics.

Turbulence and its effects are modeled by a first-order boundary layer model or by a second order turbulent kinetic energy model that uses a prognostic equation for the turbulent kinetic energy. Cloud formation, growth, and precipitation processes are simulated using bulk-water parameterization schemes. OMEGA uses a modified Kuo scheme to calculate the vertical redistribution of heat and water vapor in columns where the potential for deep convection exists. A convective parameterization scheme is used in regions of coarse resolution where the potential exists for vertical accelerations to occur. The model also includes a radiation package to approximate the effects of atmosphere and clouds on radiation.

The model incorporates an integral Aerosol Diffusion Model into the design. This Lagrangian module can follow massive and massless aerosol, with user defined source and aerosol characterization. Aerosols can be treated as discrete particles or as centroids of puffs whose dispersion is dependent on the ambient conditions. OMEGA also has the capability to transport Eulerian tracers (massless) to simulate continuous sources of gaseous material.

For more information about OMEGA the interested reader may refer to the Worldwide Web for on-line documentation describing the module and defining the variables used for OMEGA at the following address: <http://tornado.saic.com>.

Problem Statement:

An alternative to Gaussian plume models--greatly limited with their simplified assumptions--is needed to predict atmospheric dispersion. While OMEGA appears to have many advantages over current models and the Gaussian models still used by the U.S. Environmental Protection Agency, it requires validation. OMEGA must show the ability to accurately model wind flow and dispersion in various weather, terrain, and release conditions. It is recognized that no single scenario can be used to validate a model; limitations of the model will be investigated as well as strengths. Other runs would be necessitated under different conditions and different data sets.

The goals of the research are twofold. The first goal is to determine how well OMEGA can simulate the Chernobyl Nuclear Accident. The ability of the model to ingest High Resolution Analysis System data and predict deposition of Cs-137 will be tested; also, other conditions of the model such as length of simulation and treatment of wind fields will be analyzed. The second goal will be to describe OMEGA's performance with sample runs over the United States using Medium Range Forecast data provided by the National Weather Service by comparing predicted wind fields with observed weather data. Accomplishment of these goals will partially assess the validity of OMEGA to meet the needs of the Defense Nuclear Agency.

2. Literature Review

2.1 Introduction

The demand for atmospheric dispersion models comes from the need for both diagnostic and prognostic analysis concerning the space and time evolution of pollutant dispersal as a basis for public authorities to act concerning human health and the environment. Dispersion models play an important role, especially during the first stage of a pollution episode when field measurements are missing or insufficient (Desiato, 1992:2805-2806). For example, the U.S. Environmental Protection Agency (EPA) needs air quality simulation models that will estimate short-term (hours to a day) to long-term (a few days to a year) impact of source configurations.

The Chernobyl Nuclear Accident well portrayed the need for such models. On 26 April 1986, 31 people were killed and debris was scattered for miles as a cloud with radioactive particles and gases was released from the Chernobyl Nuclear Power Station (Jagger, 1991:1-10). The cloud dispersed and radioactive material was deposited throughout the Northern Hemisphere. By means of integration of environmental data, it is estimated that 10^{17} becquerels of Cs-137 were released during and subsequent to the accident (Ansbaugh et al., 1988:1513). This corresponds to less than 2 kg of Cs-137. It is estimated 17,000 will die prematurely over the next 50 years because of radiation, representing increased deaths of about 0.01%. Dosages in the Chernobyl area averaged 50 rems. Of Hiroshima survivors, about 4% received dosages greater than 100 rems

(Jagger, 1991:124-127, 222-223). For comparison, the amount of Cs-137 activity released from weapon tests of the late 1950s and 1960s is 1.5×10^{18} Bq and from the 1957 Windscale accident 4.4×10^{13} Bq (Smith and Clark, 1989:4).

The initial information on the Chernobyl release and its time variation was made available by the Soviet authorities at the International Atomic Energy Agency (IAEA) experts meeting on 25-29 August 1986 in Vienna. This included estimates of the total quantities released of a range of individual nuclides, corrected for decay until 6 May 1986 when the reactor was finally sealed, and the magnitude of their release during the first day. At the 1st Steering Committee meeting of the Atmospheric Transport Model Evaluation Study (ATMES) exercise, Dr. Petrov (USSR) provided additional information giving the daily release of Cs-137 with an estimate of the effective release height during the time after the initial release based on radiological information inside and outside the 30 km zone around the reactor, and model calculations of the material deposited (Klug, 1992:2). The release of radioactivity from the Chernobyl reactor occurred as a continuous process over a nine-day period. The initial release immediately accounted only for 25% of the total radionuclides injected into the atmosphere. After extensive analysis of the observations of radioactivity in the surroundings of the Chernobyl reactor, it was concluded that there were four distinct stages in which radionuclides were released. The initial stage was a very intensive release. During the following five days, the release rates declined steadily to a minimum value six times lower than the initial release rate. This decline in the amount of material injected into the atmosphere was then followed by a four-day period of increase to reach a level of 70% of the initial release rate. The last

stage of the process took place 9 days after the accident when the release was reduced to 1% of its initial value.

The amount released was estimated on the basis of radiation measurements and various technical analyses of samples taken from the vicinity of the Chernobyl reactor. It was concluded that about 10^{18} to 2×10^{18} Bq were discharged to the atmosphere from the core of the Chernobyl reactor. The observation indicated that about 20% of volatile radionuclides like Iodine, Cesium, and Tellurium were expelled from the damaged reactor. It is commonly accepted that the error of estimate of the Chernobyl release is $\pm 50\%$. While experimental data indicate intermittent changes in the composition of the release, as a first approximation it is assumed that each isotope varied in time proportionally to the total release (Pudykiewicz, 1990:213-225).

The atmospheric release of radionuclides following the Chernobyl reactor accident gave rise to two distinct but related activities in the field of atmospheric dispersion modeling: from a purely scientific view, it provided an opportunity to test long-range models developed for various purposes using radiological data collected through several days after the accident over Europe; it also outlined the need for operational models capable of describing in real time the long distance transport of toxic materials accidentally released into the atmosphere.

The need for a computational system to predict environmental consequences of a large-scale nuclear accident has been recognized by many countries, especially in Europe, after the Chernobyl accident. Many international agencies such as IAEA and the World Meteorological Organization (WMO) recognized the need also (Ishikawa, 1994:969).

Following the Chernobyl accident the International Nuclear Safety Advisory Group recommended IAEA should, in collaboration with WMO, review and intercalibrate models of atmospheric transport of radionuclides over short and long distances for radionuclide deposition on terrestrial surfaces and establish a data base for validation studies on models. Measurements of radioactivity performed following the Chernobyl accident provide a unique database for extensive verification studies of atmospheric models. These international agencies sponsored ATMES. The interested reader may refer to the ATMES exercise where 22 models were compared and ranked according to performance in several categories (Klug, 1992:1-10).

2.2 Elements of Atmospheric Transport Models

General requirements of any atmospheric dispersion model that calculates real-time estimates of pollutant air concentration and deposition fields are: it must use meteorological input data available in real time; it must be flexible in the range of sources, pollutants, and domains that it can consider; and it must produce results easily interpreted (Hummel et al., 1990:421-426).

One prominent example is a Gaussian emission model, probably the most widely used for estimating pollutant dispersion (Carrascal et al., 1993:147). An emission model can solve for plume rise to estimate effective height of plume from a single source. It can estimate concentrations for receptors. Source, height, emission type, and time are needed. The meteorology data needed includes wind characteristics, Pasquill Stability Classes,

temperature, mixing height, atmospheric modeling of the chemistry and physics, etc. Receptor coordinates and height are needed. Then, an estimate of concentration can be made (Turner, 1994:1-8). The Gaussian Plume Model will be discussed in a later section.

Wind data should be frequent enough so that the distance of air mass advection for one step is less than the distance between grid points. This requirement based on the simple relation between spatial variation of the wind and the length of advection of one time step. Advection beyond the next grid point will not follow the wind field if the wind field changes in the distance between grid points (unless the spatial variation of the wind is not considered in the departure point calculation).

Complex terrain models are needed for point sources to accurately calculate long-range transport, topographic effects, and aerodynamic downwash. Estimation of pollutant concentrations in areas of complex terrain is especially difficult. Under unstable conditions elevated pollutant plumes have the tendency to rise over terrain obstructions, although they may pass near the crest. Under stable conditions, plumes tend to alter their paths to flow around obstructions.

Land-water interface problems require consideration of changes in roughness and the vertical thermal structure. For instance, during spring and summer when bodies of water tend to be colder than land surfaces in the daytime, the potential exists for elevated sources in shoreline zones to fumigate for longer than the typical half-hour periods of the break-up of nocturnal radiation inversions (Turner, 1979:502-519).

In the simulation of regional or hemispheric transport, the curvature of the earth should be included. A straightforward way is to describe governing equations in

spherical coordinates. An alternative way is to project the 'spherical' computational domain onto 'flat' computational space using a conformal map projection (Ishikawa, 1994:969-978). OMEGA structures the grid such that the vertices of the grid triangles lie on the same radius of the Earth. Each grid volume is a truncated triangular pyramid with the apex of the pyramid at the center of the Earth. Thus, it uses a conformal map projection.

Another factor is the type of source. Quantities of pollutants are released from natural sources, industrial sources, mobile sources, and in many combinations. Some require models accounting for atmospheric reactions and transformations of pollutants other than in very simplistic ways.

Models predicting concentration, whether air or ground level, must include aerosol loss mechanisms such as wet and dry deposition and settling. These mechanisms are often referred to as scavenging. Dry deposition occurs as a result of gravitational settling. Rainout occurs when particles are incorporated into droplets while aerosols are in clouds.

2.3 Complications of Modelling

Modelling atmospheric dispersion with the necessary elements described in previous sections is difficult enough, but there are other complicating factors.

Mesoscale atmospheric dispersion is more complicated than smaller-scale dispersion because the mean wind field cannot be considered steady or horizontally

homogeneous over the time and space scales. Wind shear plays a much greater role: horizontal dispersion can be enhanced and often dominated by vertical wind shear on smaller scales through interaction of horizontal differential advection and vertical mixing (Moran and Pielke, 1994:96). Effects of mesoscale phenomena should be taken into account in dispersion studies, but this cannot be done without complete wind and rain field data (Rantalainen, 1993:143).

Over irregular terrain the diffusion and transport of pollutants are significantly more difficult to model than over flat terrain. The effect of the topography enhances diffusion because of increased mechanical turbulence and wind shear, and the possibility of a larger number of pollutant trajectories which are convoluted by topographic channeling and by thermally induced flows (Mullen et al., 1978:188-191).

Land-water interfaces mentioned in the previous section may be further complicated by steep planetary boundary layer (PBL) heights--some on the order of 1500 m over a grid interval of 10 km--associated with sea-breeze fronts and enhanced by the topography. In mountainous regions with large scale flows a significant horizontal shift in the maximum PBL height relative to the mountains is induced by a corresponding displacement of the thermal ridge (Lieman and Alpert, 1993:129).

2.4 Example of Models

In the course of generating models to predict weather and dispersion in the atmosphere, many different techniques have been generated. It is interesting to compare

some of these methods and see the limitations and benefits derived from them with OMEGA.

The traditional source-oriented approach consists of solving model equations forward in time for given emission sources of pollutant to obtain a time and space distributed concentration field. It allows calculation of various air pollution characteristics for any number of receptors. For any new emission scenario, however, the model solution must be repeated (Uliasz et al., 1994:104).

With any grid, available data does not lie directly on the grid points. A common method is to interpolate to the model grid at each observation time by an optimal interpolation method. The spatial weighting function is based on the estimation variance of the interpolated data obtained from this method. If an observation is located precisely at a model grid point, $W = 1$, and if a model point is sufficiently distant from the observation location, $W = 0$; otherwise, the weight varies depending on spatial distribution and number of observations.

The following subsections under 2.4 describe eight different models. The Newton relaxation method describes a means of predicting flow fields using limited amounts of data. The Gaussian Plume Model is described since it is generally used by the U.S. EPA. The Air Resources Laboratory (ARL) model demonstrates means of predicting deposition. The remaining models were used in the ATMES exercise and presented for comparison.

2.4.1 Newton Relaxation

Newton relaxation used to predict flow fields have two major advantages. One is its conceptual simplicity and low computational demand. Another is it produces a flow field that is a combination of the predicted and observed variables when and where the observations may occur. In data sparse regions, only the model governing equations are used to predict the flow field. In theory, continuous four-dimensional data assimilation should be superior to mass-consistent diagnostic models that simply interpolate the wind field in three dimensions into data sparse regions. Spatial and temporal interpolation techniques employed by these models may result in significant wind speed and direction errors, especially in highly complex terrain.

The disadvantages of Newtonian relaxation are: 1) the coefficient of relaxation is a guess; and 2) assimilation of local or unrepresentative components can occur (i.e., microscale observations may be spread over a relatively large area). For instance, local influence of a valley floor observation can be spread up the valley walls (Fast and O'Steen, 1994:310-311).

2.4.2 Gaussian Plume Models

For a Gaussian emission model assuming continuous emission, mass conservation, and steady-state, the crosswind/vertical concentration distance is given by using the standard deviations of plume distribution for all directions: σ_x , σ_y , and σ_z . These values depend on the weather parameters and stability classes. The Gaussian distribution is given by the ordinate value as shown in Figure 1.

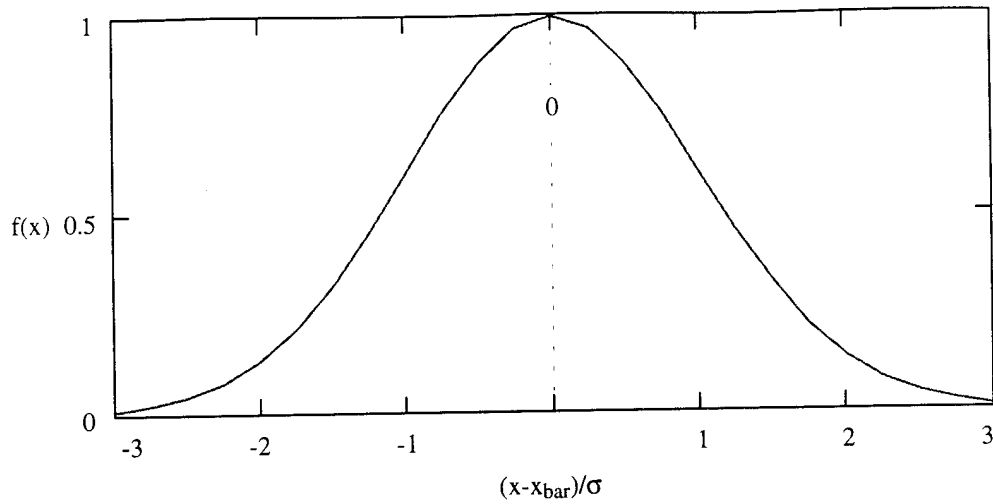


Figure 1. Gaussian Distribution Curve.

(Turner, 1994:2-1, 2-4).

In its simplest form, the Gaussian plume equation for downwind concentrations at ground level is written:

$$\chi(x,y,z=0) = Q [\pi u \sigma_y \sigma_z]^{-1/2} \exp[-(y^2/\sigma_y^2 + H^2/\sigma_z^2)]/2,$$

where $\chi(x,y,z=0)$ is ground-level concentration at downwind distance x and crosswind distance y , u = mean wind speed, Q = source intensity, H = effective height of release, and σ_y and σ_z are lateral and vertical coefficients of dispersion. Plume rise and coefficients of dispersion can seldom be measured, which forces one to resort to the use of empirical formulae, of which there are many proposed. The variability inherent in these parameters warrant careful consideration of any Gaussian model, and it is perhaps advisable to carry out runs using several of the best-performing sigma sets (e.g. the Brigg's Formulae perhaps most widely used) to get a feel for the range of variability to be expected (Carrascal, 1993:147, 156). In a report, Pasquill reminded the U.S. EPA to make the best use of Gaussian modeling through specific measurements relating closely

to dispersion. He reemphasized the use of standard deviation of the wind direction angle determined over 1-hr periods.

Accuracy of Gaussian plume models are limited by several factors. Errors in the emission rate will propagate directly into an error in the calculated concentration. Since wind speed generally increases with height above the ground, estimation of the wind speed at the point of release may be in error on the order of 10 to 15 percent. Since the effective height of release is dependent upon wind speed and stack parameters, it may also have errors of up to 20 to 25 percent. Dispersion parameters found by Pasquill stabilities and Pasquill-Gifford dispersion parameters consider the atmosphere in six classes, while in reality it is a continuum. Considerably different concentrations are calculated with a change of one stability class in the assumptions. Larger errors are expected with extremes of stability and large distances.

At the source of release, slight errors in the estimation of wind direction can result in tremendous errors of concentration where the problem is to estimate the concentration at specific locations. Often in this case the magnitude of the highest downwind concentrations under stated stability and wind speed are estimated quite well, but the location may be in error. Therefore, it is important to make exceptionally good estimates of the wind direction for each time period or expect to put up with large error bounds, perhaps as much as a factor of ten.

Gaussian models are good for estimation, but their application is limited by the assumptions not applying to many release scenarios and by the accuracy in measuring the

model parameters. Its simplicity and ability to predict many short term velocities by a normal distribution are still attractive (Turner, 1994:2-13, 2-15, 5-1).

2.4.3 Air Resources Laboratories (ARL)

ARL developed a computerized model to calculate transport, diffusion, and deposition of effluents on regional and continental scales. Each puff diffuses according to:

$$C_m = (Q/2p\sigma_h^2 Z_m) \exp(-R^2/2\sigma_h^2)$$

where C_m is ambient air concentration in the mixed layer, Q is emission amount per puff, σ_h is horizontal standard deviation, Z_m is height of the mixed layer, and R is distance from puff center. The concept of a deposition velocity is used to calculate dry deposition along a trajectory and an empirical scavenging ratio is used for wet deposition. The fraction of mass removed from the mixed layer by dry deposition is:

$$C_m V_d dt / C_m Z_m$$

where V_d is the dry deposition velocity and dt is the time interval at which puff concentrations are calculated (Heffter and Ferber, 1990:400-407).

2.4.4 WSPEEDI

The Worldwide version of System for Prediction of Environmental Emergency Dose Information (WSPEEDI) was revised to include terrain following vertical coordinates with compressibility of the atmosphere being considered. A particle dispersion model is used to simulate the atmospheric transport of radionuclides. The

radioactive plume is expressed by a mass of particles with separate calculations for the position of each particle. The equations incorporate effects of eddy diffusion and horizontal diffusion to describe particle movements.

WSPEEDI was a participant in the ATMES exercise. The computed surface air concentration of Cs-137 was directly compared with measurements at 18 sites. Agreement is generally good in Central Europe and Kozanice (Greece). At some sites in Western Europe, the simulated results correspond to the measurement well during several days after the arrival, but the computed concentration decreases rapidly after that. This rapid decrease was due to the westerly winds which prevailed over these areas bringing in clean air after May 3. This suggests the possibility the plume reached further west than simulated. The uncertainty reveals the difficulty in pinpointing values of deposition, which greatly depend on local precipitation (Ishikawa, 1994:969-978).

2.4.5 Canadian Tracer Model

Extensive development work with a three-dimensional (3-D) tracer model was conducted by the Canadian Meteorological Center. The new model was tested on the Chernobyl case using objectively analyzed meteorological fields over a period of one month. The major limitation of the system used in these studies was the use of observed meteorological fields. Thus, the development of a predictive version of the tracer model is a natural continuation of previous work.

The models which simulate atmospheric tracers are relatively complex because of the need to represent a wide range of physical and chemical processes. To simulate the

interaction between meteorological processes and atmospheric transport of nonconservative species, one needs a set of thermodynamic equations coupled with the mass conservation equations for atmospheric tracers. The system in the most general form is as follows:

$$dU/dt = F - (1/\rho) \nabla p - \Pi U \quad (1)$$

$$d \ln \rho / dt = - \nabla \cdot U \quad (2)$$

$$dT/dt = A_T (L/c_p) Q - (L/c_p) E_0 \quad (3)$$

$$p = \rho R T \quad (4)$$

$$dq/dt = -Q + E_0 \quad (5)$$

$$dm/dt = Q - (P - E_r) - E_0 \quad (6)$$

$$dn^i/dt = S^i(n^i, \dots, n^M, m, T) \quad (7)$$

(I = 1, ..., M)

Where the symbols have the following meanings:

U--velocity field, F-mass forces, p-atmospheric pressure, Π - operator representing turbulent mixing, ρ -density, ∇ - gradient operator, T-temperature, R-gas constant, q - mixing ratio of water vapor, L - latent heat constant, A_T - dynamic part of tendency rate for temperature, Q - latent heat of condensation, E_0 - evaporation, m - cloud water, P - precipitation rate, E_r - evaporation of rain, n^i - mixing ratio for atmospheric trace species, $S^i(\cdot)$ - source and sinks for atmospheric trace species, d/dt - material derivative ($d/dt = \partial/\partial t + U \cdot \nabla$), M - number of atmospheric trace species simulated in the model.

The system (1)-(7) consists of $(8 + M)$ equations and simulates the meteorological processes and chemical reactions of atmospheric trace species. The boundary conditions for the dynamic and chemical part of the system have to be specified, and they depend on the particular geometry of the domain being considered.

The first eight equations of the system are in fact a non-hydrostatic meteorological model. The model equations include the bulk representation of microphysical processes such as condensation, the formation of clouds and precipitation and the evaporation of rain. The atmospheric boundary layer processes are represented by the operator Π which takes into account the momentum transfer by convective processes and by dynamically generated turbulence. The set of Eq. (7) represents a nonlinear atmospheric chemistry. The set given by Eqs. (1)-(7) is designed mostly for application on a regional scale and is far too complex for most applications involving the simulation of atmospheric processes in a hemispheric or global scale. One common simplification is to assume hydrostatic equilibrium in a tracer model driven by a primitive equations meteorological model.

These simplifications affect calculations of turbulent vertical fluxes of momentum, heat and moisture in the surface layer, and scale horizontal mixing. Stable precipitation is currently calculated by removing the excess of moisture above some threshold value of relative humidity. The moist convection is parameterized. Cloud cover required in the calculation of radiative heating is obtained as a function of the local relative humidity. Surface temperature in the spectral model is calculated by solving an energy balance equation over land; over water, surface temperature is obtained from climatological data. Wet scavenging is represented by a statistical parameterization.

The source term for Chernobyl, Q^i , was approximated using the concept of the 3-dimensional virtual source. The release in this approximation is represented by a function of three spatial variables and time:

$$Q^i(\eta_x, \eta_y, \sigma, t) = (E^i(t) F(\sigma) / 2\pi\sigma_H^2) \text{Exp}[-r^2/2\sigma_H^2] \quad (8)$$

where:

$E^i(t)$ -- amount of radioactivity released

$$F(\sigma) = f(\sigma) \cdot \left(\frac{R \cdot T}{\sigma \cdot \pi} \right) \cdot \left[\int_{\sigma_T}^{\sigma_B} \frac{f(\sigma) \cdot R \cdot T}{g \cdot \sigma} d\sigma \right]^{-1}$$

$f(\sigma)$ - function describing the vertical distribution of the release

(η_x^0, η_y^0) - coordinates of the source of the release

$$r = ((\eta_x^0 - \eta_x)^2 + (\eta_y^0 - \eta_y)^2)^{1/2}$$

σ_H - standard deviation of the horizontal mass distribution

σ_B, σ_T , are values at the bottom and top of the domain, respectively

R - specific gas constant of air

T - temperature

The effective release was a function of time with height changing from 4000 m just after the explosion to 1500 m subsequently. The initial height of 4000 m was assumed to be in direct response to the initial explosion. The smaller vertical extension of 1500 m which was assumed during the days following the accident mostly reflects the intensive convection over the burning reactor and subgrid-scale vertical mixing of radioactive material in the lower part of the troposphere.

The tracer was solved initially using data stored in the archiving system of the Objective Analysis at the Canadian Meteorological Center. The analysis of meteorological fields at the time of the accident was performed every 6 hours on a Gaussian latitude-longitude grid with a resolution of 128*32 points over the Northern Hemisphere. The meteorological fields for intermediate time levels were obtained by time interpolation.

The verification of the results from the diagnostic model was performed for a network covering the Northern Hemisphere and indicates that the simulation was quite accurate. Predicted times of arrival and the times of arrival of maximum activity agree quite well with the observed values. The ratio of the calculated and observed values varies between 0.21 and 2.80 with a mean value of 1.05.

The results of the diagnostic calculations indicate that during the first two days following the Chernobyl accident, the radioactive cloud was transported mostly towards Scandinavia. A second southern segment of the cloud had spread southeastward over the Black Sea in the direction of the Middle East. On April 29, a well developed westerly flow began to transport radioactive material across the former USSR.

The 2 day prediction has relatively good accuracy, as the model was quite good in predicting the main directions of the transport. The quality of the 4 day prediction, however, deteriorated substantially. The deficiency of the predictive model is manifested mostly by the lack of radioactive material over western Europe. The first run of the predictive model showed good prediction on a regional scale for the first 2-3 days after the release (Pudykiewicz, 1990:213-225).

Another approach to Chernobyl involved replacing the usual Pasquill dispersion coefficients (sigmas) for the simplified Gaussian plume diffusion approach in this terrain with dispersion coefficients related empirically to the terrain roughness and atmospheric turbulence. A steady state modeling approach is used; neglect of transport time simplifies the model considerably but causes the model to overreact to changes in meteorology when modeling receptors are long distances from the sources. In spite of this shortcoming, the model predicts reasonably well for all averaging times (Mullen et al., 1978:188-191).

2.4.6 MATHEW

A Lagrangian, mass-adjusted, three-dimensional wind field model (MATHEW) was developed to provide wind fields for a pollutant transport model (ADPIC). The two basic boundary conditions imposed on the field are constant mass flux and zero mass flux corresponding to reflection on the boundaries (Klug, 1992: 68). The wind model incorporates terrain explicitly, is site independent, uses available meteorological measurements, is stable, and calculates three-component velocities at a large number of grid points. Constant air density was assumed, but variable air density can be included with little modification.

Comparison of results with field data taken during tracer releases shows the model calculations to be within a factor of 2 in 50% of the comparisons and within an order of magnitude for 90% of the tests. Examination of model calculations shows the root-mean-square errors to be 10% in wind speed and 5-10° in wind direction, except near

topographic barriers where the errors increase to follow flow around and over the terrain features (Sherman, 1978:312-319).

2.4.7 MEDIA

This model involves numerical schemes that can deal with advection and diffusion processes without distortion by numerical effects. Pollution concentration is advected by the wind field as predicted by the operational coupling model. To simplify the procedure, the diffusion is modeled using exchange coefficients. It means pollutant is assumed to be diffused in the same way as water vapor.

Sinks for the model are treated as follows: Wet deposition due to scavenging by precipitation is computed using a global coefficient of air-to-water transfer, which roughly describes dilution or catching. Dry deposition is modeled using a coefficient dimensionally equal to a deposition velocity multiplied by the concentration in air near the ground. Radioactive decay is another sink. Diffusion is modeled on a subgrid scale by a Gaussian distribution. On the six sides of the integration area (four lateral sides, top of the atmosphere and ground level) boundary conditions are treated as outgoing fluxes according to Orlanski (1976).

The data used was from the European Centre for Medium Range Weather Forecasts. Time-evolution was according to a step function as described in the Technical Specifications Document of the ATMES Report.

Results were very satisfactory for all but one location. Problems with monitoring stations close to the accident may be the result of linear interpolation over 6 hours of large-scale meteorological fields or errors in knowledge of the source term.

Sensitivity tests were performed on the model. A space resolution of 2×2 degrees did not result in a great loss of quality on the average values. Reducing the time step to 1 hour instead of 3 hours did not notably improve the results. Reducing horizontal diffusion leads to a great loss of quality on the smaller values without any benefit for the extrema; increasing it leads to smooth minima and maxima. The chosen value seemed best.

Sensitivity to deposition velocity is rather important and shows it is necessary to know and accurately describe the characteristics of the transported material and underlying surface over which it will be deposited. Omitting rainfall gives almost the same results for ambient concentration. This can be explained by the fact that during the 10 days after the accident, the radioactive cloud was seldom affected by washout. Average concentrations in air are not the best indicators since the average losses due to washout is low compared to the amount of pollutant released during such a short time (Piedelievre et al., 1990:1205-1220).

2.4.8 LORAN

LORAN (Long range atmospheric advection of nuclides) makes use of horizontal wind field varying linearly in time and space. The advection velocity for the current time interval dt at point (x,y) for the given geopotential height used is calculated via linear

interpolation of the corner point values and for the times t_1 and t_2 . A typical value of dt is 1 hr.

Dry and wet deposition is evaluated by means of an average deposition value for each pollutant or nuclide used in the simulation. In principle, deposition velocity should depend on atmospheric turbulence and surface resistance. The long duration of the release, however, and the lack of information on surface resistance, has prompted the use of the value of 0.003 m/s. Scavenging of contaminated air by rain is described by a scavenging coefficient times the concentration.

Results of the comparison for air show a constant overestimation of the concentration. This can be explained by the fact that a considerable fraction of the source did not travel to long distances from the release point. Results for cumulative deposition show good agreement in the two cumulative distributions of results. The overall bias for deposition again indicates overestimation.

The model LORAN would have been among the best had it participated in the ATMES exercise. It is believed that its good performance is mainly due to its prescription of the mixing layer growth. Results of the comparison of cumulative deposition data are very different when data close to the source point are included. This indicates that the model does not behave well close to the source; probably due to the simple assumption on the constant reference level and on instantaneous air mixing in this level. The model actually seems to perform better if Russian deposition data is not included (Galmarini et al., 1992:143-154).

2.5 Evaluation of Models

Model accuracy is difficult to determine since it depends upon both the ability of the model to simulate the physics of the atmosphere and the accuracy of the input information. Most evaluations contain the product of these two effects. Although a comparison between model estimates and measurements may verify a model, a good result may be due to compensating errors in various portions of the model. Thus, independent verification of portions of the model is highly desirable. The comparison may be subjective by displays of scatter plots or quantitative such as deriving various statistics from data sets. The use of laboratory data and numerical simulations of dispersion is stressed because they can be repeated to generate well-defined ensemble-mean concentration fields.

Two questions of plume dispersion models are of primary concern: 1) How well does a model predict the high ground-level concentrations; 2) Is the model based on sound physical principles and give good predictions for the "right" reasons?

There are two major steps in a model physical evaluation. The first is an assessment of the scientific formulation and modeling assumptions for the physical problem of interest. The second is an evaluation of model predictions using measurements from laboratory and field experiments.

Many different forms of tests are used for model evaluation. Performance evaluation tests the performance under different conditions through a partitioning of the

data. Sensitivity testing determines the changes in model output due to specific changes in an input parameter (Turner, 1979:502-519).

A key step in evaluation is separating the model error--the difference between the observed and predicted values of concentration--from the variability and other sources of concentration variance. This is best done through a residual analysis in which one examines the statistics of the residual between the observed and predicted concentrations. The key objective in residual analysis is to show the difference exhibits no trends with any of the ensemble variables (Weil, 1994:224).

The following statistical tests are used for comparison of model results with actual data: True difference, normalized true difference, absolute difference, absolute fractional bias, variance of true difference, variance of fractional bias, mean square error, and correlation coefficient (Ciolek, 1994:237-238).

Model evaluation for the Chernobyl Nuclear Accident is based on the comparison between the following observed and computed analysis: Cs-137 air concentration samplings paired in space and time; time-integrated concentrations at each locality; time of arrival of the cloud. The model simulation and consequently all the analysis are limited to the first 12 days after the beginning of the release, i.e., until 24:00 GMT on 7 May.

The APOLLOS model defined the computed arrival time of the cloud at a certain location as the beginning of the first time step at which the Cs-137 concentration exceeds a threshold value CT; the observed arrival time is defined as the initial time of the sampling interval with measured concentration exceeding CT. A threshold value

$CT = 0.1 \text{ Bq m}^{-3}$ was chosen, with the exception of a few sites whose first measurement was higher than 0.1, for which $CT = 1 \text{ Bq m}^{-3}$. Due to large uncertainty of the observed arrival time and the unavoidable arbitrary and inhomogeneous choice of the threshold, this part of the study is intended to give only a rough indication of the model capabilities of estimating the time of transport of the cloud.

There are several potential reasons for inaccuracy of model results when a long-range and long-duration dispersion episode like the Chernobyl release is simulated. Among others, the most important are perhaps the prescription for source rate and shape, the three-dimensional wind field used for calculating the particle trajectories, the parameterizations of boundary-layer height and the horizontal diffusion, the treatment of the cloud scavenging by dry and wet deposition. Besides, the relative weight of each of these sources of uncertainty strongly depends on the method used for comparing the results.

After several air quality model evaluation exercises involving a large number of source scenarios and types of models, it is clear that the magnitudes of the uncertainties in model predictions are similar from one application to another. For example, when considering continuous point sources and receptors at distances of about 0.1 km to 1 km downwind, uncertainties in ground-level concentration predictions lead to typical mean biases of about ± 20 to 40% and typical relative root-mean-square errors of about 60 to 80%. It is not uncommon to see overprediction by 50% at one site and underprediction of 50% at a second site for two otherwise identical model applications. This fundamental

level of model uncertainty is likely to exist due to data input errors and stochastic fluctuations, no matter how sophisticated a model becomes (Hanna, 1993:3).

3. Methodology

3.1 Use of Medium Range Forecast Data over the U.S.

Running OMEGA using a domain within the U.S. will provide means of verifying its ability to predict wind fields. We selected the Medium Range Forecast (MRF) data from the National Weather Service (OMEGA data processor also comes with the capability to use Nested Grid Model output and Naval Oceanographic Global Atmospheric Prediction System (NOGAPS) data from Fleet Numerical and Oceanographic Center, or hand entered data). The data includes actual measurements at 0000Z of the day of interest with predictions for 1200Z and 2400Z. The ability of OMEGA to predict wind fields for the domain of interest will depend, in part, on the accuracy of the later time MRF predictions.

The domain of interest spans 36.5° N by 43.5° N and 80.25° W to 89.75° W (see Figure 2 on the next page for a view of the domain). These ranges were chosen to make best use of the 10 km resolution terrain data included with the model while presenting reasonable run times for the workstation. The days covered the 16th through the 18th of September, 1995. These were chosen because of a trough seen in the wind flow. The boundary conditions will then have wind field in basically the same direction, but the domain (with wind fields generated by OMEGA) will not yet account for the trough. The ability of OMEGA to generate the trough within the boundary will partially validate its ability to predict wind fields.

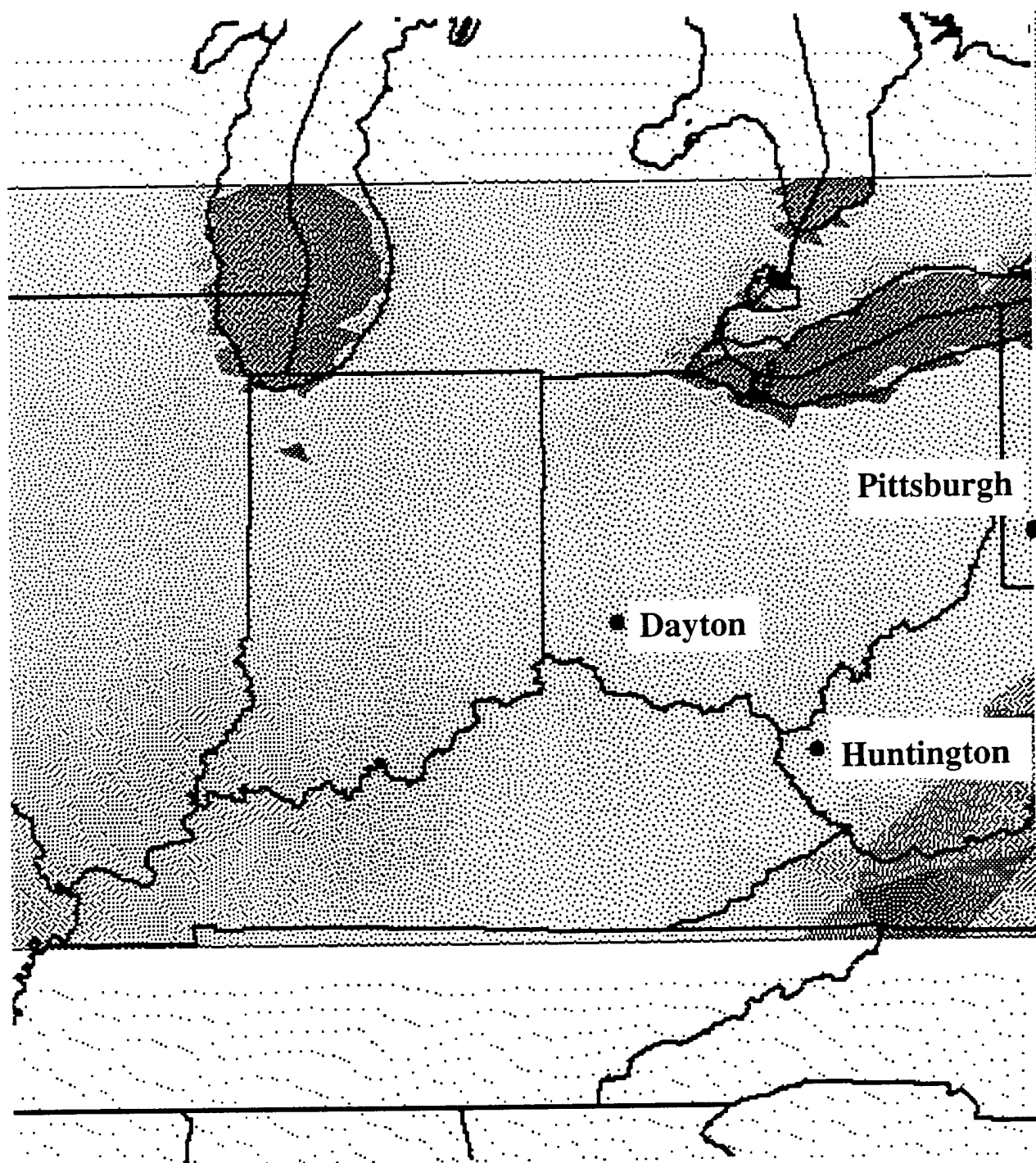


Figure 2. Domain of MRF Data Run.

OMEGA is run three separate times with one day of MRF data per run. This involves analysis data at 0000Z and forecast data at 1200Z and 2359Z. Later, the run may be repeated using the boundary conditions for each of the cases in sequence over a longer period. This makes use of analysis data alternating with forecast data every twelve hours. We expect the latter run to be more consistent with analysis data because more of the boundary conditions use analysis data. The general flow of the actual weather patterns and the velocity will be compared with OMEGA predictions at four levels. Assessment at the 300, 500, 700, and 850 mb levels at each station at twelve-hour intervals leads to 80 data readings. OMEGA predictions involve interpolation because the layers do not exactly correspond to these pressures. Therefore, a third-order Lagrangian polynomial using two data points on either side of the value desired was selected to obtain the values for wind speeds.

The means of assessing the predictions of OMEGA comes through a two-tailed t-test. The weather stations in the domain available for us from the National Weather Service analysis maps are Dayton, OH; Huntington, WV; and Pittsburgh, PA. The resolution of the winds from the analysis maps is 2.5 knots and the resolution of the direction is about 10° . The u and v components estimated from the analysis map vectors are then compared with the predictions of OMEGA. The test chosen reflects use of paired data and the null hypothesis chosen was that the mean of the wind speeds was equal for the predicted wind and actual winds. A 95% confidence interval was chosen with the null hypothesis rejected when the limits set by the t-value was exceeded.

3.2 Verification with HIRAS Data and the Chernobyl Nuclear Accident

3.2.1 Background from HIRAS USAFETAC Climatic Database Users Handbook No. 5 (October 1988:3, 8)

Assessment of OMEGA will also come through verification with Chernobyl data. The model of choice is HIRAS data, or High Resolution Analysis System, generated and obtained from archives at OL-A, Air Force Combat Climatology Center (AFCCC). The data is recorded at six-hour intervals and involves only analysis data. A disadvantage, however, is the limitations in the 1986 data as described later in this section. Use of all analysis data would lend more credibility to the ability of OMEGA to predict wind fields based on observed data rather than forecast data.

OMEGA does not support use of archived HIRAS data (the newer data is in a different format and would be used in future scenarios), thus requiring a special data preprocessor. HIRAS produces global upper-air analyses on a 2.5° by 2.5° latitude/longitude grid. All standard pressure levels are available. HIRAS uses a variety of observations taken from land stations, ships, buoys, aircraft, RAOBs, PIBALs, and satellites. HIRAS analyzes five elements--heights, u- and v-component winds, temperature, and relative humidity--directly; all other HIRAS elements are derived from these five.

HIRAS has two main components: a "first-guess" and an analysis model. HIRAS uses an analysis technique called "optimum interpolation", or OI. This model is an adaptation of the analysis used at the National Meteorological Center. OI takes into

account three factors: 1) distance between observations and grid points; 2) accuracy of the observing instruments; and 3) expected accuracy of the first-guess value.

Distance between observations and grid points is incorporated by assigning weights to observations surrounding each grid point. In HIRAS, these weights decrease exponentially with distance. Each observation is allowed to affect the first-guess analysis depending on how close it is to the grid point. If a grid point has observations nearby, the first-guess value is corrected; otherwise, it remains unchanged.

The second factor manifests a major advantage of OI. It assigns every instrument type a unique "expected error" that has been determined statistically. The basic OI rule is that the lower the expected instrument error, the more weight that the observation will receive.

The last factor is accuracy of the first guess. Each HIRAS analysis produces two types of fields: analyses and errors. Analyses are the standard grid-point analyses previously discussed. Error fields, however, are specialized fields unique to OI. The error fields are used as "running" standard deviations, and indicate how accurate the analysis is at each grid point. The more observations available, the better the analysis and the lower the expected error. Over data-rich areas like North America and Europe, error values are low.

HIRAS upper-air analysis provides all the initial conditions for AFCCC models, especially the Global Spectral Model. The main purpose of an initialization scheme is to control imbalances in initial conditions which cause development of motions (like gravity waves) that the model cannot resolve. These perturbations could be real (from micro- or

sub-grid scale phenomena) or fictitious (from small observational errors). Nearly every numerical forecast model uses some form of initialization to compensate for these.

Quality control applied at AFCCC includes manual and automated checks. Forecasters perform the manual checks by adding bogus observations or deleting real observations. If they believe anything to be erroneous while reviewing the first-guess model output, forecasters can introduce artificial data for use in subsequent analysis. For example, if they think the first-guess has moved an upper-air trough too far east, artificial data may be introduced to move it back to where it belongs.

Automated quality control is directed at throwing out bad observations. The first steps are when HIRAS compares each observation with the first-guess analysis. If an observation grossly disagrees with the first-guess (defined to be when the difference between the observed value minus the first guess value exceeds the analysis error field for the analysis point under consideration by more than eight error standard deviations), it is immediately rejected. If an observation just barely passes the gross checks, it is flagged and submitted to a second procedure that compares it with a nearby observation. If one of these flagged observations significantly disagrees with its neighboring observation (defined to be when the difference between the two values is more than four times the analysis error at the analysis point being considered), it is rejected.

There are some known problems with data that exist for the Chernobyl case. Moisture analyses are not from HIRAS, but from the old MULTAN model. Data elements vorticity, precipitable water, dew point depression, and relative humidity are not available. This should not affect the performance of the OMEGA model but prevents a

method of checking the model performance. Surface temperature is actually an extrapolation from the 1,000-millibar temperature analysis. This data is not surface temperature and should not be used as such. In addition, surface elements u-wind, v-wind, and specific humidity are not available.

3.2.2 Atmospheric Transport Model Evaluation Study (ATMES) Requirements

Validation using Chernobyl Nuclear Accident data ideally would follow the requirements stated in the Technical Specification Document used for the ATMES exercise. The exercise encompassed the European region between 100° W to 40° E and 35° N to 70° N. A smaller area was addressed in the ATMES exercise by limits 4° E to 36° E and 43° N to 62° N. Model results were requested for a 14 day period, with model starting time reflecting the Chernobyl source term data viewed as a step function. Estimated effective height of the initial plume center-of-mass is also given. Models predicted several parameters including surface air concentration, arrival times for Berlin and Munich, and Cs-137 deposition rates.

3.2.3 Methods Used for OMEGA

The domain chosen for OMEGA validation will allow a proof-of-concept. The grid chosen was 10° E to 34° E and 47° N to 62° N (see Figure 3 on next page). This was chosen to include in the domain most of the area of deposition found in the first four days. The resolution chosen was 30 to 80 km using the stretchable horizontal grid. This is comparable to resolutions used by ATMES exercise participants. The HIRAS data used for the model was from 25 April 1986, 00Z, to 29 April 1986, 00Z. Modeling the

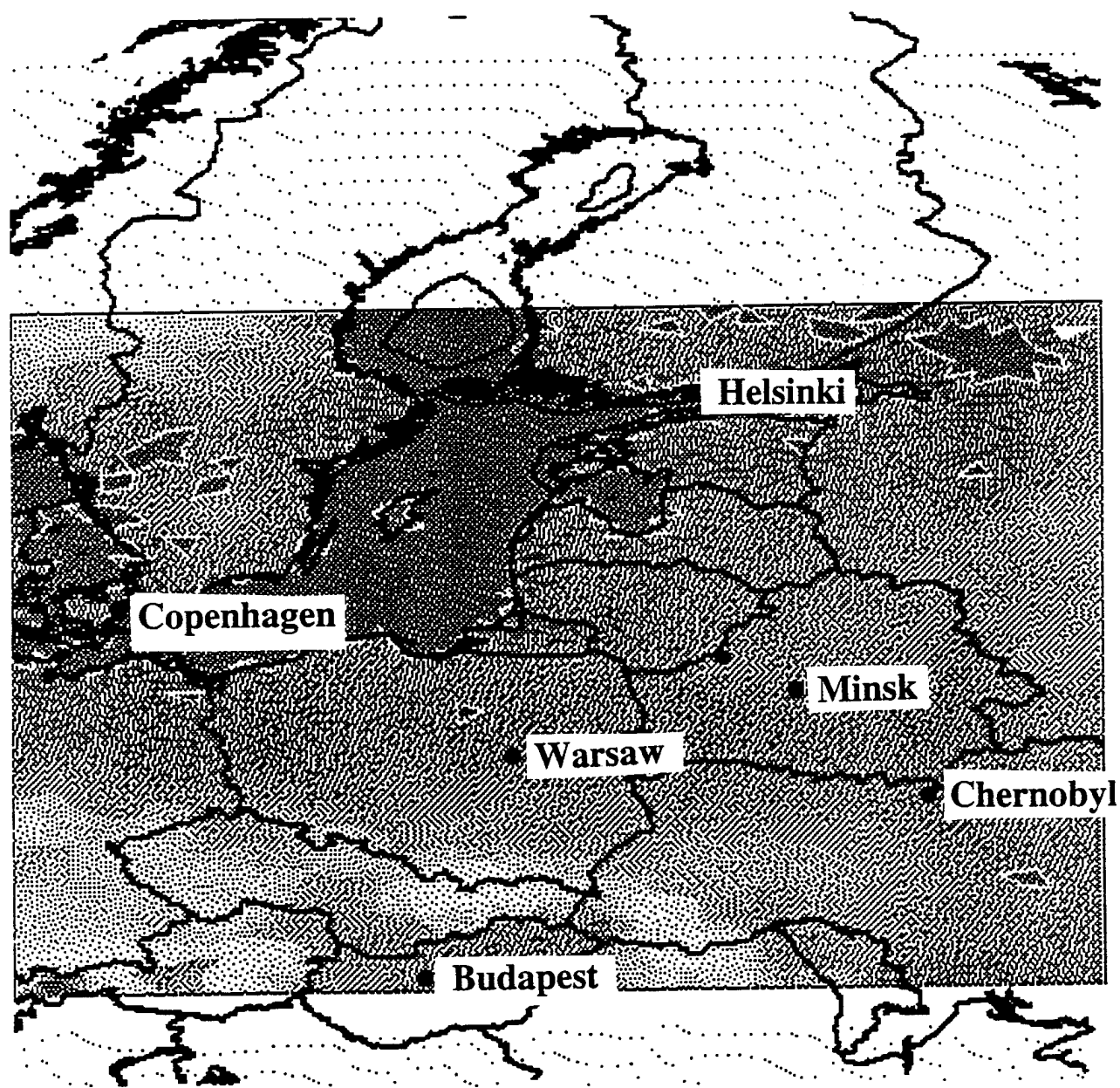


Figure 3. Domain of HIRAS Data Run.

source term required writing a Fortran 90 program according to the ATMES Technical Specifications Document.

Several factors required a limited scope for the Chernobyl validation. The number of cells in OMEGA is limited to around 6,000. In order to keep the resolution comparable to other models, the domain must be constrained. The existing IBM AIX system runs approximately the same length of time as the simulation time for this part of the validation. Output files generated every hour require 12 MB of space. Also, the data files run through the preprocessor took great disk space. These constraints limited the area of domain and the duration of the simulation.

Limitations in the OMEGA model itself would not easily lend it to the comparison of ATMES. As mentioned in the first chapter, OMEGA has different ways of tracking releases. The puffs released would follow Lagrangian treatment in tracer mode of the model. This would track the centroid of the puffs but require extensive integration to determine the concentration along each time step and the amount deposited to the ground. This prevented use of the user defined source term as intended, but further efforts to validate OMEGA may make use of the code (see Appendix D). The Eulerian tracer capability permits release of a specified concentration and allows it to disperse, but this mode does not support a varying release source required to simulate Chernobyl. Therefore, the validation is limited to proof-of-concept that the wind fields generated and the deposition footprint predicted by the tracers show the capability to adequately portray a release such as Chernobyl.

The analysis of the wind fields is similar to that of the runs over the U.S. Values used, though, are at ground level, 850 mb, and 500 mb, and only at 00Z at each day. The following cities were chosen: Budapest, Copenhagen, Minsk, Helsinki, and Warsaw, as wind field maps from the Täglicher Wetterbericht (daily weather bulletin) allowed determination of wind velocity most readily for them. Resolution for these maps were 2.5 km/h in wind speed and about 10° in direction. Comparison of wind speeds will follow the same methodology used with the run over the U.S. with separate paired t-tests for u and v wind components.

4. Results of OMEGA Validation

4.1 Medium Range Forecast Data Validation

Wind field predictions from September 16-18, 1995, were compared against actual analysis. Using the 80 verification points, the direction was within one compass location (e.g., if the true direction was west, this would include west-northwest and west-southwest) in 56 of the cases. General wind field patterns seem qualitatively to predict the winds accurately. For the complete list of comparisons, please refer to Appendix B.

An assessment of the magnitudes was also performed, with the components of the predicted wind fields and the analysis wind fields compared in a paired t-test. Using a 95% confidence interval, the values of u-component were not statistically different in the two sets. The mean value of the analysis values was 17.8 and the mean value of the predicted values was 19.0. The t-value was -0.99. The values of v-component were also not statistically different. The mean of the analysis values was -2.2 and the mean value of the predicted values was -2.6. The t-value was 0.45. This leads us to accept the null hypothesis that the two sets are the same. (Rejection occurs with a t-value greater than 2.0 or less than -2.0.) Root-mean-square errors for the data were approximately 10 knots for u-component and 9 knots for v-component. This is good considering errors from the instruments measuring these winds are on the order of 6.5 knots.

Upon breakdown of the weather data, more bad data points come from inclusion of the station at Pittsburgh. A separate paired t-test run without Pittsburgh data showed good comparability. The 54 data points were compared using the paired t-test, resulting

in a t-value of -0.52 and p-value of 0.61 for u-component, showing excellent similarity. An identical number of v-component data points were compared, resulting in a t-value of -0.33 and p-value of 0.74. Therefore, the indication is choosing stations along the boundary cells produce worse results. This is to be expected with noise from the boundary conditions affecting the wind fields.

Another arrangement of the data was made leaving in all three weather stations, but removing the 300 mb data. The 60 data points were compared using the paired t-test, resulting in a t-value of -0.80 and p-value of 0.43 for u-component. The values for the v-component were -0.15 and 0.88, respectively. We also expect the higher wind field assessments to contribute to error because of larger velocities and proximity to the upper boundary level affecting the domain.

Figures 4-6 show the errors for the wind field predictions based on the output from OMEGA and National Weather Service maps. National Weather Service maps at 850 mb and OMEGA generated wind fields are shown in Appendix C. The data points represent the National Weather Service observations with components derived from the maps. The difference between the observed values and the predicted values is plotted.

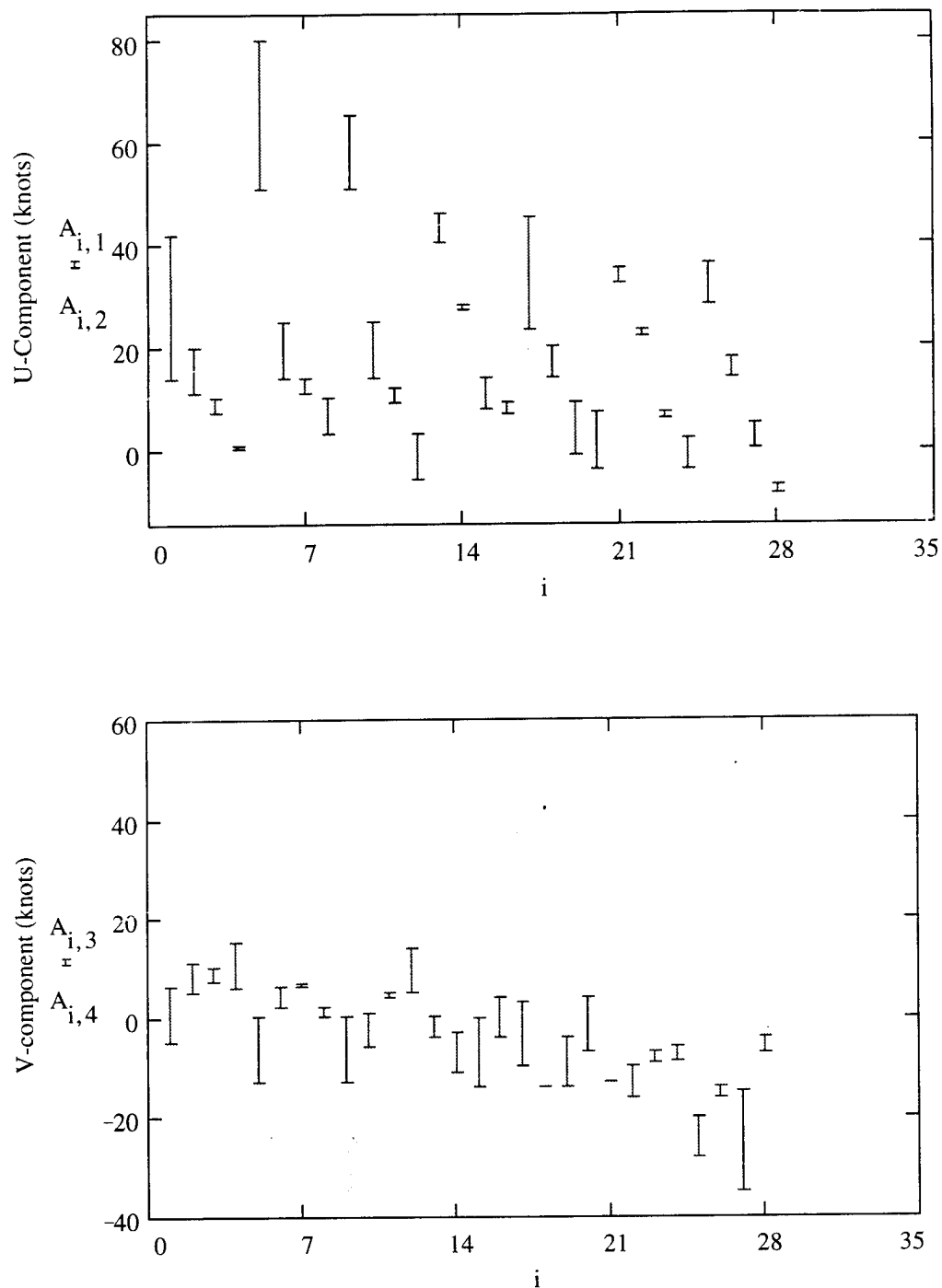


Figure 4. Error plot vs case number of (a) u-component and (b) v-component wind speeds for Dayton, Ohio from 16-18 September, 1995, beginning 00Z at 12-hour intervals. Points 1-7 are at 300 mb; 8-14 are at 500 mb; 15-21 are at 700 mb; 22-28 are at 850 mb.

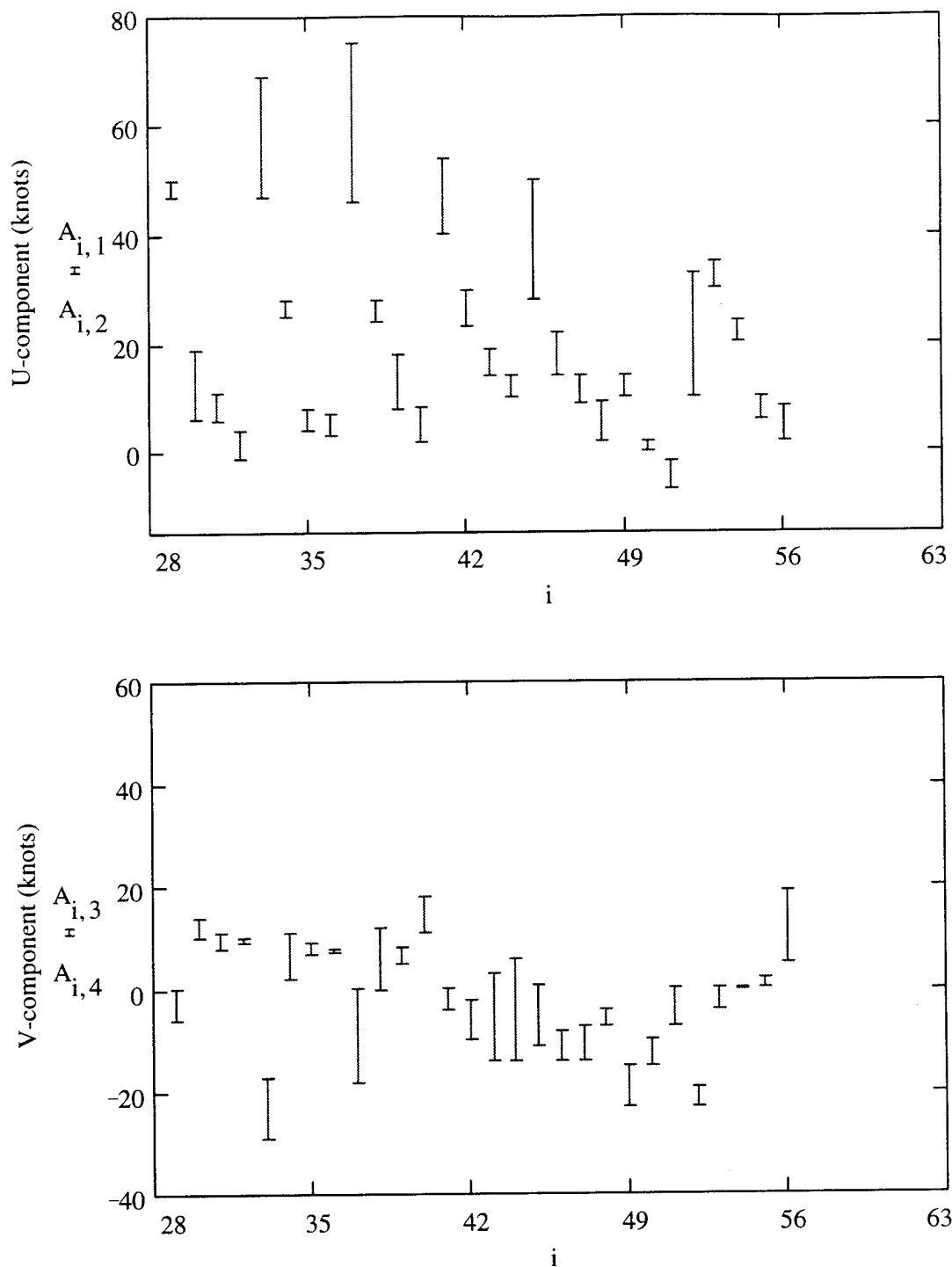


Figure 5. Error plot vs case number of (a) u-component and (b) v-component wind speeds for Pittsburgh, PA from 16-18 September, 1995, beginning 00Z at 12-hour intervals. Points 29-35 are at 300 mb; 36-42 are at 500 mb; 43-49 are at 700 mb; 50-56 are at 850 mb.

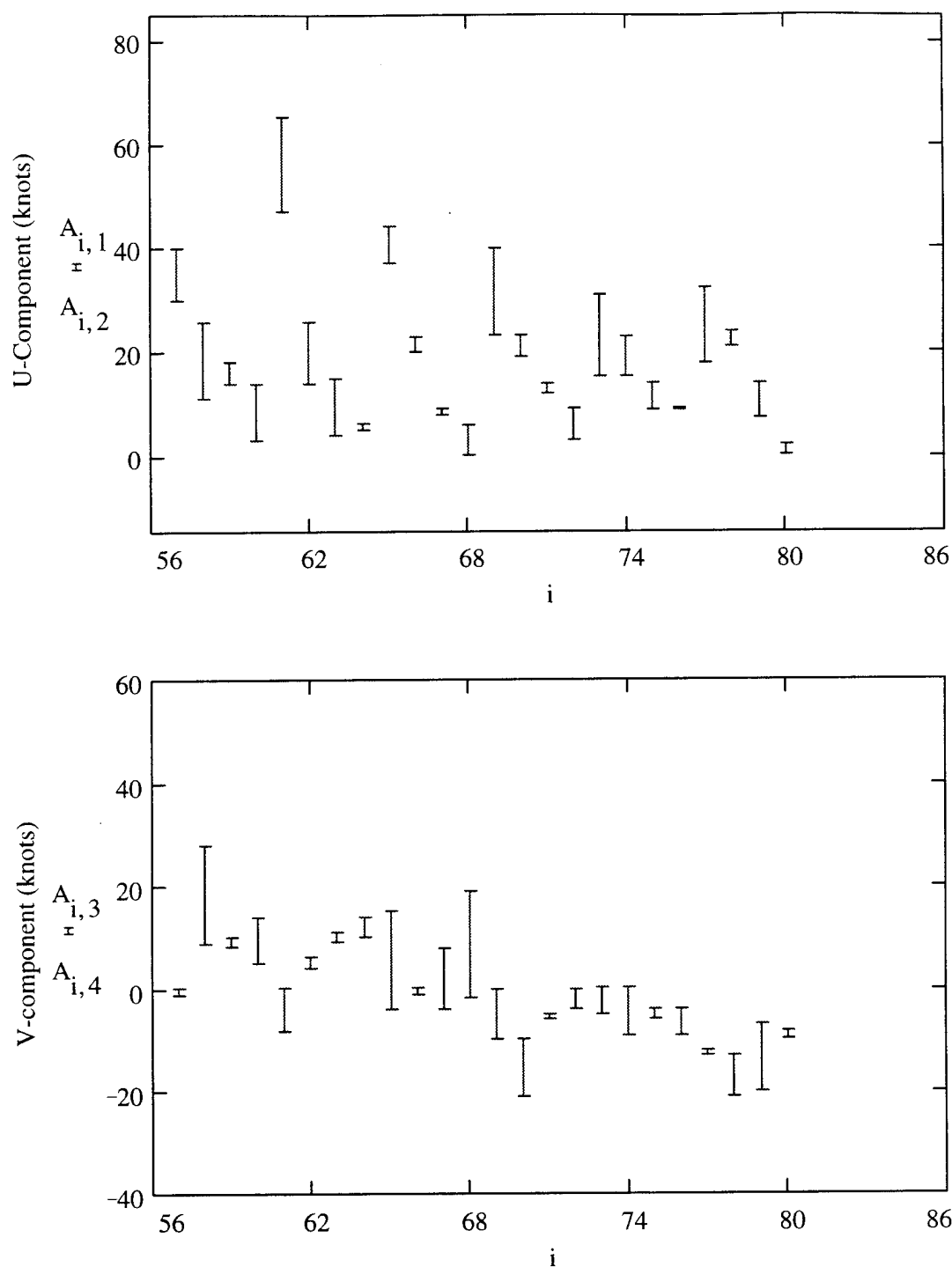


Figure 6. Error plot vs case number of (a) u-component and (b) v-component wind speeds for Huntington, WV from 16-18 September, 1995, beginning 00Z at 12-hour intervals. Points 57-62 are at 300 mb; 63-68 are at 500 mb; 69-74 are at 700 mb; 75-80 are at 850 mb.

4.2 High Resolution Analysis System Data Validation

Wind field predictions from April 25-28, 1986, were compared against analysis maps from the Täglicher Wetterbericht. There were 60 cases of paired data. In only 25 of the cases, the predicted wind direction was within one compass location of the analysis. General wind field patterns seem to predict winds accurately, though, as much complicated wind flow affected the area during this time. For a complete list of comparisons, please refer to Appendix B.

An assessment of magnitudes was performed using components of predicted wind fields and analysis wind fields compared in a paired t-test. Using a 95% confidence interval, the values of the u-component were not statistically different in the two sets with a t-value of -0.79. The values of the v-component were also within the 95% confidence interval, but with a value of 1.95, just below the rejection value of 2.0. The root-mean-square values are also worse than the case with MRF data, with error values of 15 knots for u-component and 11 knots for v-component.

Since the data from 28 April 1986 was suspected of being faulty, a separate test was performed for 25-27 April 1986, leaving 45 data points. The u-component t-value was 0.37 with a p-value of 0.71, excellent comparison. The v-component t-value was 1.54 with a p-value of 0.13. The rms error was approximately 10 knots for u-component and 8 knots for v-component, comparable to the results with MRF data.

On the following page, Figure 7 shows the results from the run over Europe. The data points represent the difference between components derived from daily weather maps and predicted values.

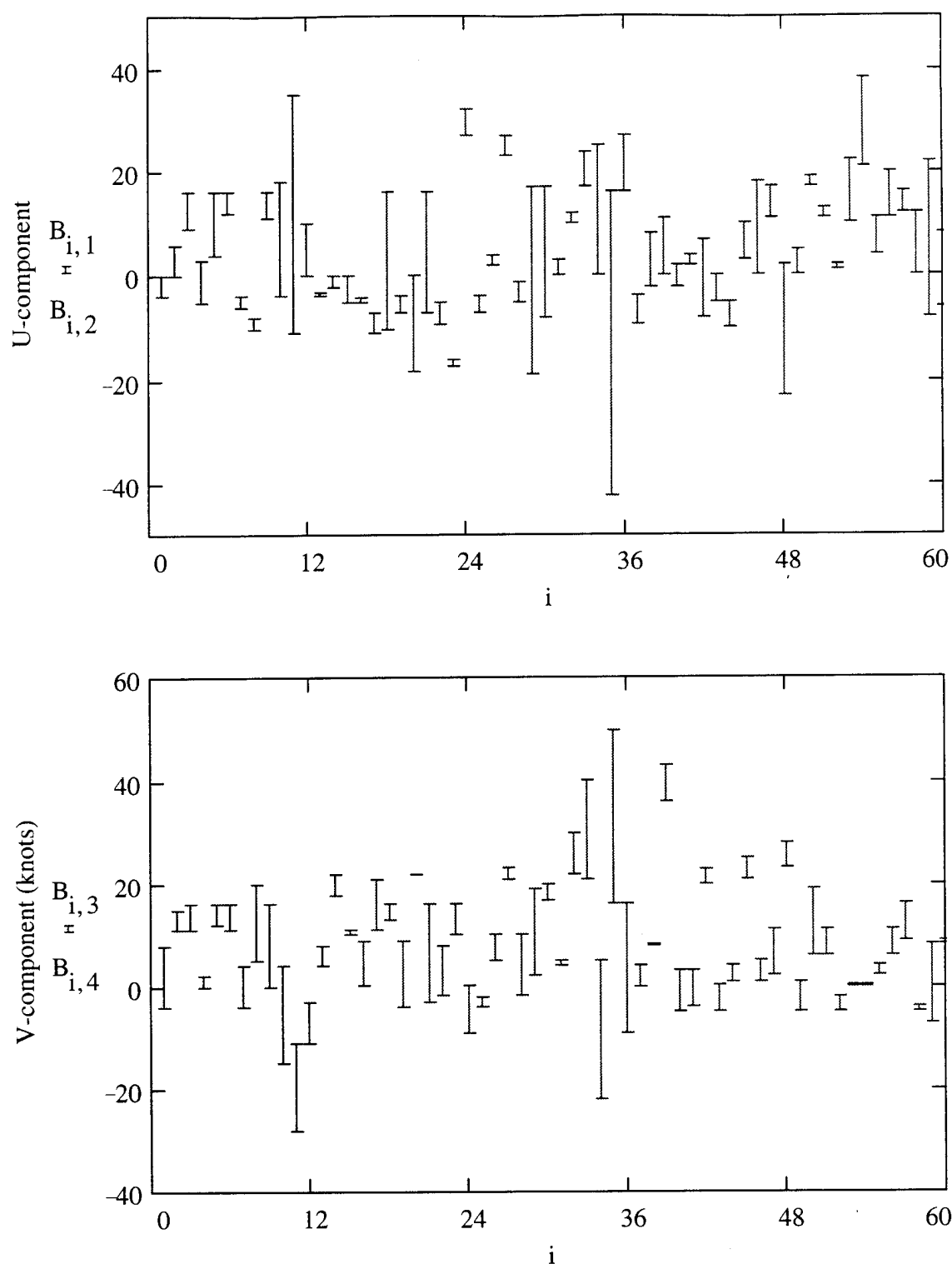
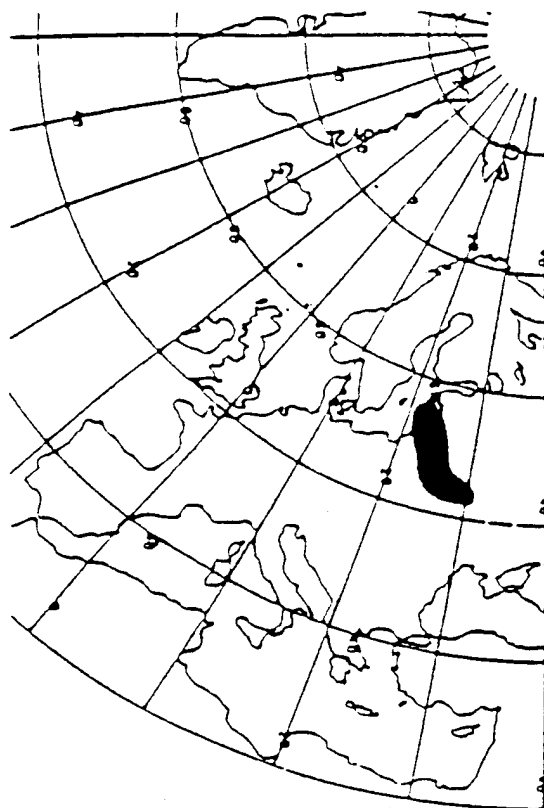


Figure 7. Error plot vs case number of (a) u-component and (b) v-component wind speeds over Europe from 25-28 April, 1986, all at 00Z. Points 1-12 are for Budapest; 13-24 are for Copenhagen; 25-36 are for Helsinki; 37-48 are for Minsk; 49-60 are for Warsaw.

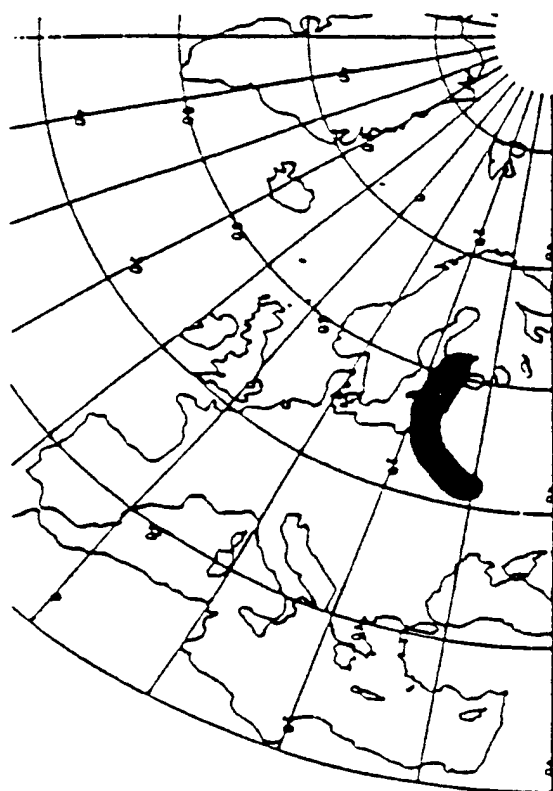
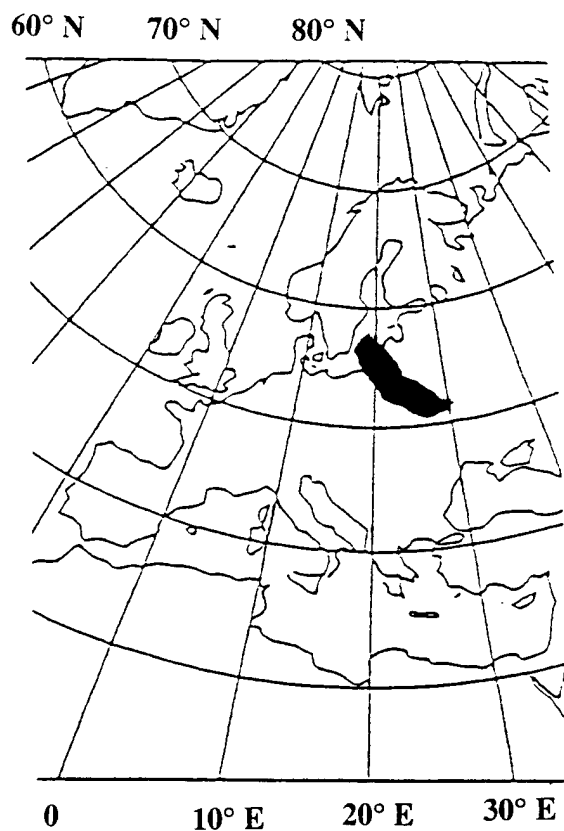
With such drastic changes in wind flow in this region, the resolution of the domain itself would lend difficulty to predicting winds at a particular location and time. Running the model for more than one day continuously generated an increasing error wave in the w-component winds in the upper portion of the domain, which generally add to the error in the domain. The predictions matching the wind direction were generally in the first two days of the run.

The most important factor, however, seemed to be the data for 28 April 1986. Unrealistic pressures under 900 mb at the surface were predicted throughout the domain, and vertical wind speeds of over 120 knots were predicted. This was the case regardless of when OMEGA started, and casts suspicion on the data itself. These errors begin on 28 April, 1986, and the model is unable to recover. These errors were present whether or not a source term was incorporated in the model.

Prediction of general wind flow patterns qualitatively seems reasonable. Deposition predicted from the Eulerian tracer capability was compared to actual deposition maps shown in Figures 8 and 9, where the maps for predicted deposition were derived from the model. Appendix D shows the deposition maps actually produced by OMEGA. As mentioned earlier, this provides a proof-of-concept that OMEGA could reliably predict the deposition, but concentrations are, unfortunately, not available. An assumption with the qualitative assessment is the dispersion of the tracer would generally follow the same distribution but differ by an unknown factor.



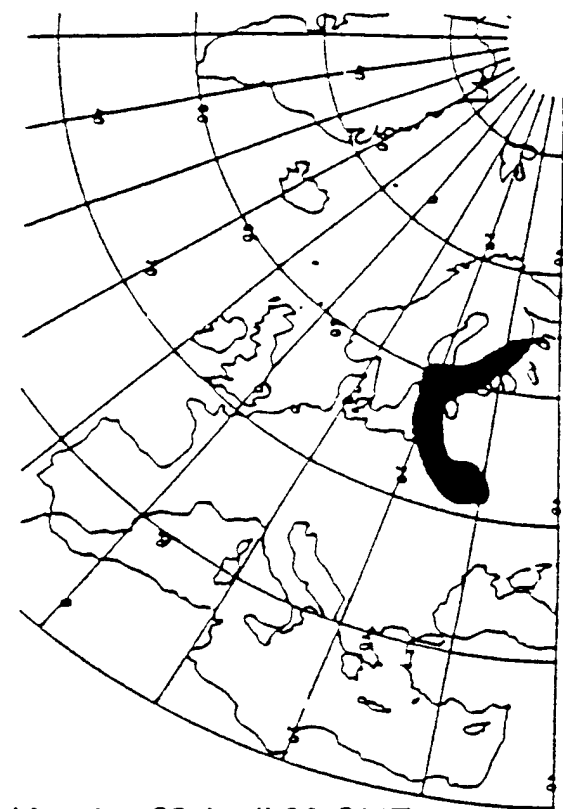
Sunday 27 April 00 GMT



Sunday 27 April 12 GMT



Figure 8. Actual deposition maps (Smith, 1989:11) (left) compared to OMEGA derived footprint for a 1500 meter release height.



Monday 28 April 00 GMT



Figure 9. Actual deposition map (Smith, 1989:11) (left) compared to OMEGA derived concentration at 300 mb for a 1500 meter release height.

4.3 Comment on Results

The size of the domain selected allows only a proof-of-concept and not a full comparison with the ATMES exercise participants. The smaller area selected makes the boundary conditions more critical and provides OMEGA with a more stringent test of its ability to predict wind fields.

Comparison of the wind fields using a paired t-test does not reflect the standard meteorology test using root-mean-square errors, but it does indicate how OMEGA performs overall in prediction of the wind fields. Deposition predictions depend less upon the short-term variations in the wind field than longterm projections, as seen by the pattern for deposition, which compares well for the first 48 hours after the release. As a means to compare with meteorological models, values for rms errors seem very reasonable for MRF data but seem high for HIRAS data

The runs shown indicate the potential of OMEGA to fulfill the needs of the Defense Nuclear Agency. A fuller analysis at this time is not practicable as the model is currently under revision. Some enhancement to the model such as inclusion of a varying source with Eulerian tracers, capability to resume the model, and capability to use larger domains would be required in order to use the same validation method used in ATMES. As mentioned in the literature review, two runs cannot validate the model. The model would require runs under various scenarios to permit the confidence in it required for assessment of limitations and accuracy. These runs do show the promise and unique features of OMEGA at work.

5. Conclusion

5.1 Achievement of Objectives

The primary goal of the research was to determine how OMEGA performs ingesting HIRAS data and predicting deposition from a variable release source term such as found in the Chernobyl Nuclear Accident. The intermediate goal was to describe OMEGA's performance with sample runs over the United States using MRF data by comparing wind fields with weather data. These goals would partially assess the validity of OMEGA to meet the needs of the Defense Nuclear Agency.

The results are favorable. OMEGA has the capability to ingest data in various formats through its preprocessor to predict wind fields and meteorological conditions. The domain size and length of simulation permitted are also adequate for a proof-of-concept validation of its capabilities. Limitations with the means of tracking particles do not easily lend OMEGA to predicting deposition with a variable source term, but the capability does exist and use of Eulerian tracer mode can be used to simulate a worst-case scenario likely of interest to the Defense Nuclear Agency. Based on limited comparison, prediction of wind fields was within the 95% confidence interval for both domains and data sets used.

5.2 Recommendations

OMEGA appears to satisfy the physical requirements for accurately predicting meteorological conditions. More extensive study could be taken in areas with greater

numbers of weather stations in the domain for greater statistical support for a quantitative comparison of generated wind fields with analysis data. Another option would be to compare gridded model output with gridded analysis data to increase the data.

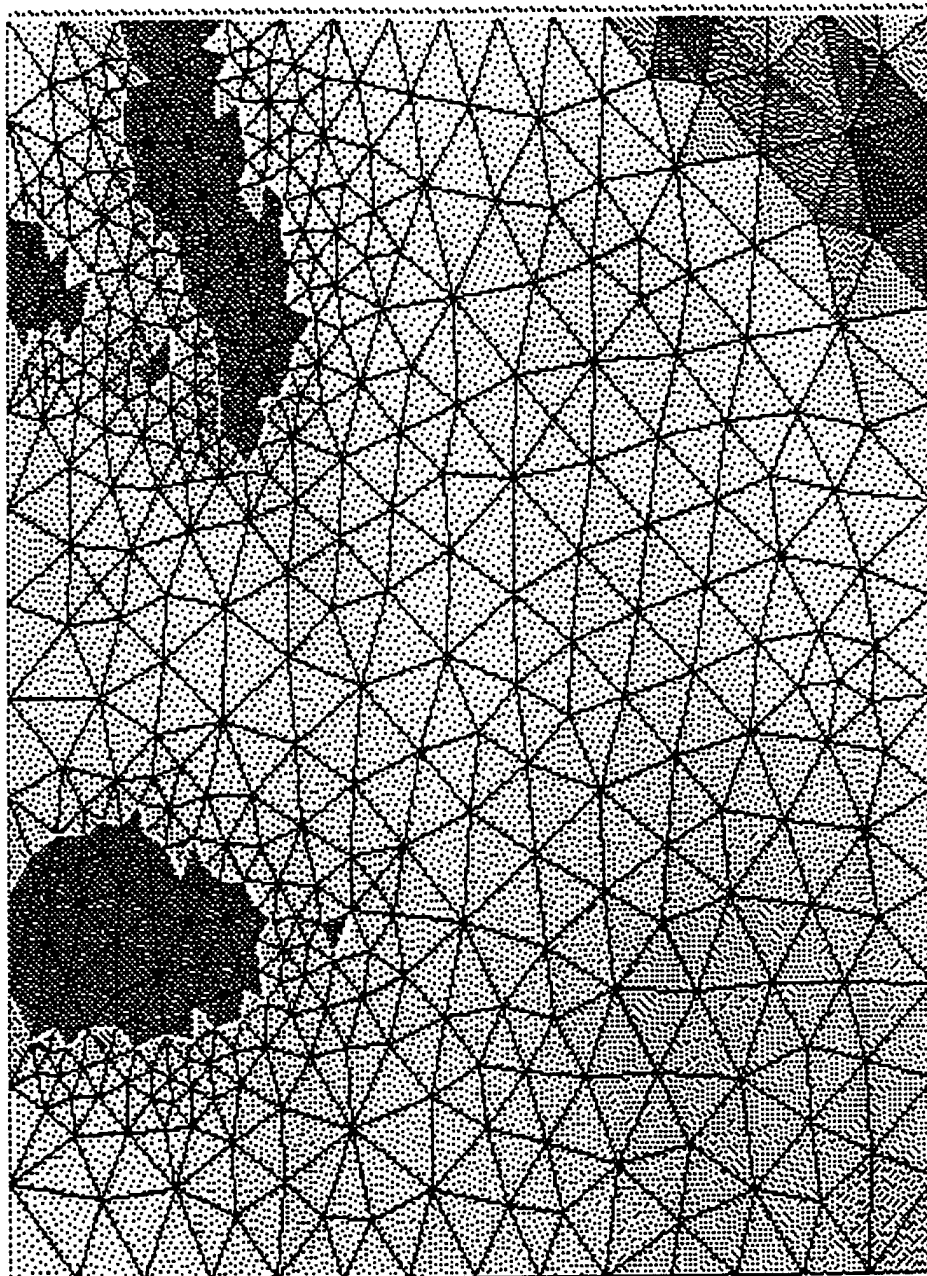
The true need, however, is to predict air concentrations and deposition values. A detailed look at the Lagrangian particles with their deviation values would allow prediction of concentration and deposition by integrating over the dispersive range of each particle along each time step (quite time-consuming). Once this is performed, it would assess the ability to forecast risk and hazard levels for variable releases, and could then be incorporated into the model's framework.

Improved user features in the model would also enhance future validation efforts. The model is limited by inability to resume after a run has completed. Future versions of the model should allow restart capability by saving wind fields, particle locations, and meteorological conditions. This would allow greater flexibility in releases and allow the most recent weather data for the model. The model could then be allowed to run for the entire release period and beyond, permitting a true means of comparison with models participating in the ATMES exercise.

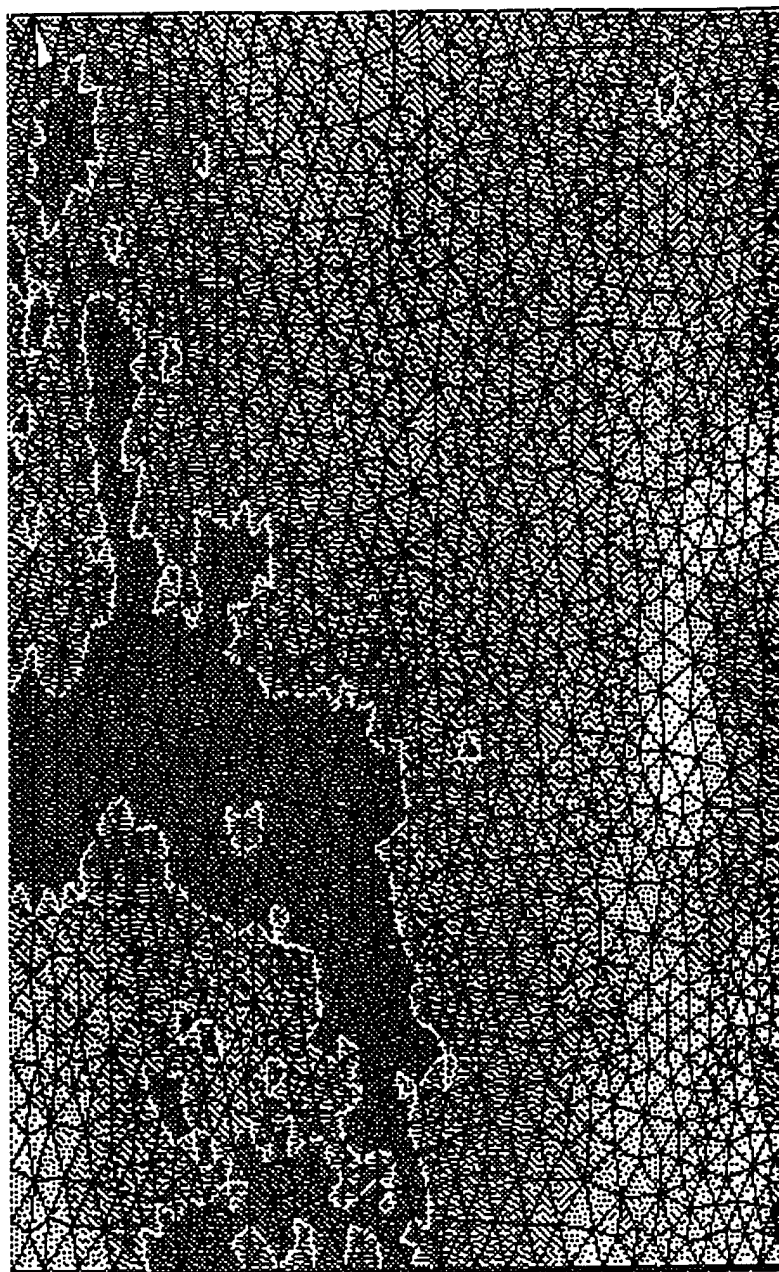
Vertical accelerations are also a concern in the wind fields. The magnitude of these accelerations surpasses reality during extended runs (and sometimes becomes suspect depending on the given data. This raises questions about the vertical layers and how the boundary conditions at the top of the domain are resolved. Further stabilization of the boundary layer at the top is necessary to prevent these unrealistic vertical accelerations.

Finally, it must be remembered that OMEGA is still under revision. The research was conducted in a manner to highlight the capabilities and strengths of the model while identifying concerns the Defense Nuclear Agency may have regarding the model's development. We have seen great improvements and impressive capabilities of the model.

Appendix A: OMEGA Generated Grids for MRF and HIRAS Validation



Grid for MRF Validation.



Grid for HIRAS Validation.

Appendix B: Wind Field Tables for MRF and HIRAS Validation

Note: Case numbers are not in the same order as the figures show.

MIDWEST

CASE	CITY	DATE	TIME	MB	U	UPRED	V	VPRED
1	DAYTON	9/16/95	00Z	300	14	42	6	-5
2	DAYTON	9/16/95	00Z	500	11	20	11	5
3	DAYTON	9/16/95	00Z	700	7	10	7	10
4	DAYTON	9/16/95	00Z	850	0	1	15	6
5	DAYTON	9/16/95	12Z	300	80	51	0	-13
6	DAYTON	9/16/95	12Z	500	14	25	6	2
7	DAYTON	9/16/95	12Z	700	14	11	6	7
8	DAYTON	9/16/95	12Z	850	10	3	0	2
9	DAYTON	9/17/95	00Z	300	65	51	0	-13
10	DAYTON	9/17/95	00Z	500	14	25	-6	1
11	DAYTON	9/17/95	00Z	700	9	12	4	5
12	DAYTON	9/17/95	00Z	850	-6	3	14	5
13	DAYTON	9/17/95	12Z	300	40	46	0	-4
14	DAYTON	9/17/95	12Z	500	28	27	-11	-3
15	DAYTON	9/17/95	12Z	700	14	8	-14	0
16	DAYTON	9/17/95	12Z	850	9	7	-4	4
17	DAYTON	9/18/95	00Z	300	23	45	-10	3
18	DAYTON	9/18/95	00Z	500	14	20	-14	-14
19	DAYTON	9/18/95	00Z	700	9	-1	-4	-14
20	DAYTON	9/18/95	00Z	850	7	-4	-7	4
21	DAYTON	9/18/95	12Z	300	32	35	-13	-13
22	DAYTON	9/18/95	12Z	500	23	22	-10	-16
23	DAYTON	9/18/95	12Z	700	7	6	-7	-9
24	DAYTON	9/18/95	12Z	850	-4	2	-9	-6
25	DAYTON	9/19/95	00Z	300	28	36	-28	-20
26	DAYTON	9/19/95	00Z	500	14	18	-14	-16
27	DAYTON	9/19/95	00Z	700	0	5	-35	-15
28	DAYTON	9/19/95	00Z	850	-9	-7	-4	-7
29	HUNTINGTON	9/16/95	00Z	300	50	47	0	-6
30	HUNTINGTON	9/16/95	00Z	500	6	19	14	10
31	HUNTINGTON	9/16/95	00Z	700	11	6	11	8
32	HUNTINGTON	9/16/95	00Z	850	4	-1	9	10
33	HUNTINGTON	9/16/95	12Z	300	69	47	-29	-17
34	HUNTINGTON	9/16/95	12Z	500	28	25	11	2
35	HUNTINGTON	9/16/95	12Z	700	4	8	9	7
36	HUNTINGTON	9/16/95	12Z	850	7	3	7.1	8
37	HUNTINGTON	9/17/95	00Z	300	75	46	0	-18
38	HUNTINGTON	9/17/95	00Z	500	28	24	12	0
39	HUNTINGTON	9/17/95	00Z	700	18	8	8	5
40	HUNTINGTON	9/17/95	00Z	850	8	2	18	11
41	HUNTINGTON	9/17/95	12Z	300	40	54	0	-4
42	HUNTINGTON	9/17/95	12Z	500	23	30	-10	-2
43	HUNTINGTON	9/17/95	12Z	700	14	19	-14	3
44	HUNTINGTON	9/17/95	12Z	850	14	10	-14	6
45	HUNTINGTON	9/18/95	00Z	300	28	50	-11	1
46	HUNTINGTON	9/18/95	00Z	500	14	22	-14	-8
47	HUNTINGTON	9/18/95	00Z	700	14	9	-14	-7
48	HUNTINGTON	9/18/95	00Z	850	9	2	-4	-7
49	HUNTINGTON	9/19/95	00Z	500	10	14	-23	-15
50	HUNTINGTON	9/19/95	00Z	700	0	2	-10	-15

MIDWEST

51	HUNTINGTON	9/19/95 00Z	850	-2	-7	0	-7
52	HUNTINGTON	9/19/95 12Z	300	10	33	-23	-19
53	PITTSBURGH	9/16/95 00Z	300	30	35	0	-4
54	PITTSBURGH	9/16/95 00Z	500	20	24	0	0
55	PITTSBURGH	9/16/95 00Z	700	10	6	0	2
56	PITTSBURGH	9/16/95 00Z	850	8	2	19	5
57	PITTSBURGH	9/16/95 12Z	300	30	40	0	-1
58	PITTSBURGH	9/16/95 12Z	500	11	26	28	9
59	PITTSBURGH	9/16/95 12Z	700	18	14	8	10
60	PITTSBURGH	9/16/95 12Z	850	14	3	14	5
61	PITTSBURGH	9/17/95 00Z	300	65	47	0	-8
62	PITTSBURGH	9/17/95 00Z	500	14	26	6	4
63	PITTSBURGH	9/17/95 00Z	700	4	15	9	11
64	PITTSBURGH	9/17/95 00Z	850	6	5	14	10
65	PITTSBURGH	9/17/95 12Z	300	37	44	15	-4
66	PITTSBURGH	9/17/95 12Z	500	20	23	0	-1
67	PITTSBURGH	9/17/95 12Z	700	9	8	-4	8
68	PITTSBURGH	9/17/95 12Z	850	0	6	-2	19
69	PITTSBURGH	9/18/95 00Z	300	23	40	-10	0
70	PITTSBURGH	9/18/95 00Z	500	23	19	-10	-21
71	PITTSBURGH	9/18/95 00Z	700	14	12	-6	-5
72	PITTSBURGH	9/18/95 00Z	850	9	3	-4	0
73	PITTSBURGH	9/18/95 12Z	300	15	31	0	-5
74	PITTSBURGH	9/18/95 12Z	500	15	23	0	-9
75	PITTSBURGH	9/18/95 12Z	700	14	9	-6	-4
76	PITTSBURGH	9/18/95 12Z	850	9	9	-4	-9
77	PITTSBURGH	9/19/95 00Z	300	32	18	-13	-12
78	PITTSBURGH	9/19/95 00Z	500	21	24	-21	-13
79	PITTSBURGH	9/19/95 00Z	700	7	14	-7	-20
80	PITTSBURGH	9/19/95 00Z	850	0	2	-10	-8

USSR

CASE	CITY	DATE	MB	U	UPRED	V	VPRED
1	BUDAPEST	4/25/86	500	11	13	11	6
2	BUDAPEST	4/25/86	850	19	17	19	6
3	BUDAPEST	4/25/86	1021	0	5	-5	1
4	BUDAPEST	4/26/86	500	38	21	0	0
5	BUDAPEST	4/26/86	850	22	10	0	0
6	BUDAPEST	4/26/86	1033	2	1	-5	-2
7	BUDAPEST	4/27/86	500	16	12	16	9
8	BUDAPEST	4/27/86	850	11	20	11	6
9	BUDAPEST	4/27/86	1021	4	11	4	2
10	BUDAPEST	4/28/86	500	8	-6	8	9
11	BUDAPEST	4/28/86	850	-8	22	8	-7
12	BUDAPEST	4/28/86	896	0	12	-5	-4
13	COPENHAGEN	4/25/86	500	0	11	43	36
14	COPENHAGEN	4/25/86	850	8	-2	8	8
15	COPENHAGEN	4/25/86	1030	-4	-9	4	0
16	COPENHAGEN	4/26/86	500	-8	7	20	23
17	COPENHAGEN	4/26/86	850	4	2	-4	3
18	COPENHAGEN	4/26/86	1037	2	-2	-5	3
19	COPENHAGEN	4/27/86	500	10	3	25	21
20	COPENHAGEN	4/27/86	850	-10	-5	4	1
21	COPENHAGEN	4/27/86	1030	0	-5	0	-5
22	COPENHAGEN	4/28/86	500	-23	2	23	28
23	COPENHAGEN	4/28/86	850	11	17	11	2
24	COPENHAGEN	4/28/86	884	0	18	5	1
25	HELSINKI	4/25/86	500	23	27	23	21
26	HELSINKI	4/25/86	850	4	2	10	5
27	HELSINKI	4/25/86	1049	-4	-7	-4	-2
28	HELSINKI	4/26/86	500	-8	17	20	17
29	HELSINKI	4/26/86	850	-19	17	19	2
30	HELSINKI	4/26/86	1048	-5	-1	-2	10
31	HELSINKI	4/27/86	500	17	24	40	21
32	HELSINKI	4/27/86	850	12	10	30	22
33	HELSINKI	4/27/86	1035	0	3	5	4
34	HELSINKI	4/28/86	500	16	27	16	-9
35	HELSINKI	4/28/86	850	16	-42	16	50
36	HELSINKI	4/28/86	899	0	25	5	-22
37	MINSK	4/25/86	500	0	-5	11	10
38	MINSK	4/25/86	850	0	-2	22	18
39	MINSK	4/25/86	1023	-4	-3	4	8
40	MINSK	4/26/86	500	16	-10	16	13
41	MINSK	4/26/86	850	-11	-7	11	21
42	MINSK	4/26/86	1032	-5	-4	0	9
43	MINSK	4/27/86	500	16	-7	16	-3
44	MINSK	4/27/86	850	0	-18	22	22
45	MINSK	4/27/86	1017	-4	-7	-4	9
46	MINSK	4/28/86	500	32	27	0	-9
47	MINSK	4/28/86	850	-16	-17	16	10
48	MINSK	4/28/86	891	-5	-9	-2	8

USSR

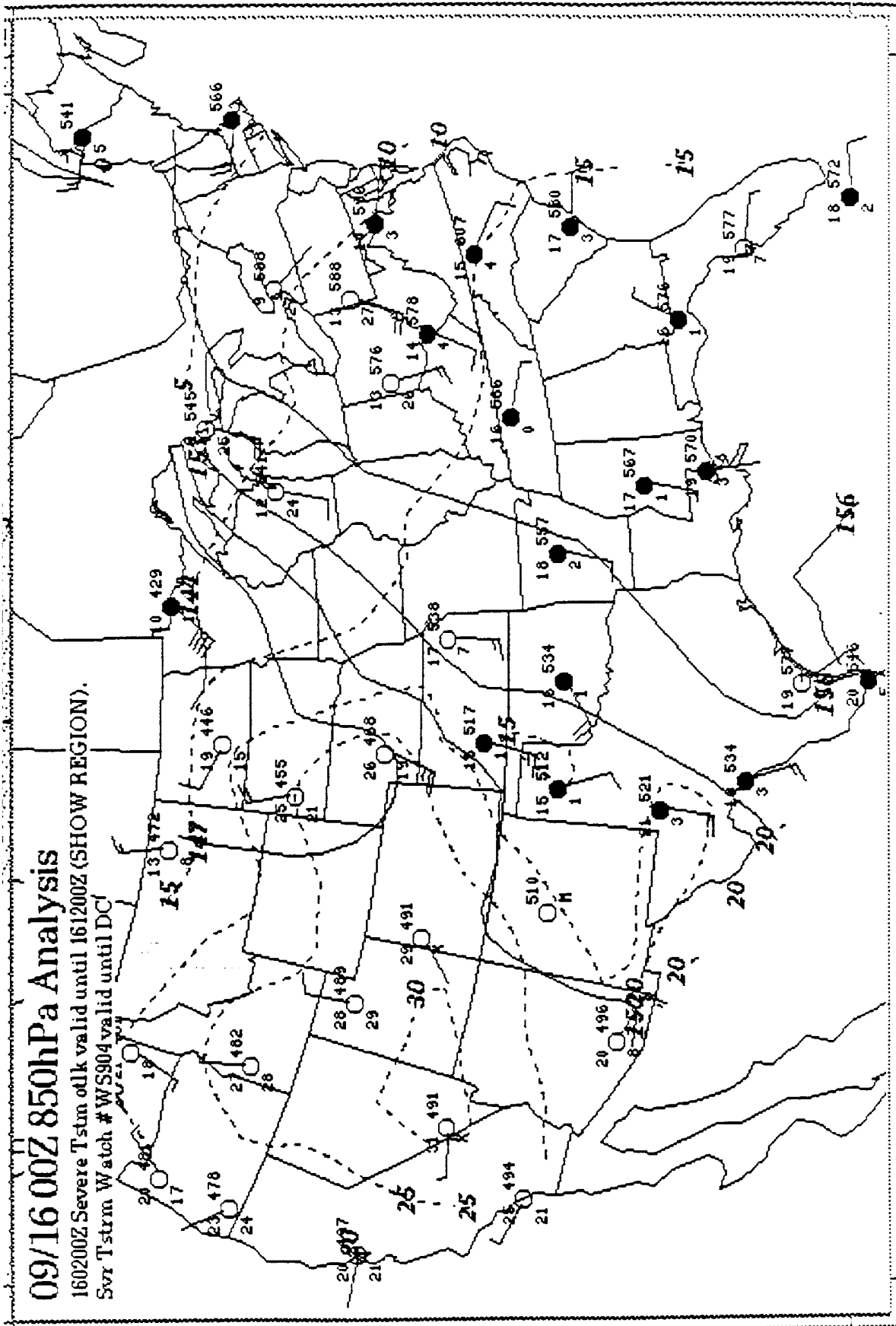
49	WARSAW	4/25/86	500	16	9	16	11
50	WARSAW	4/25/86	850	0	6	11	15
51	WARSAW	4/25/86	1014	-4	0	-4	8
52	WARSAW	4/26/86	500	16	12	16	11
53	WARSAW	4/26/86	850	16	4	16	12
54	WARSAW	4/26/86	1032	-5	3	2	0
55	WARSAW	4/27/86	500	16	11	16	0
56	WARSAW	4/27/86	850	-8	-10	20	5
57	WARSAW	4/27/86	1015	-4	-6	-4	4
58	WARSAW	4/28/86	500	0	10	-11	-3
59	WARSAW	4/28/86	850	-11	35	-11	-28
60	WARSAW	4/28/86	895	-4	18	4	-15

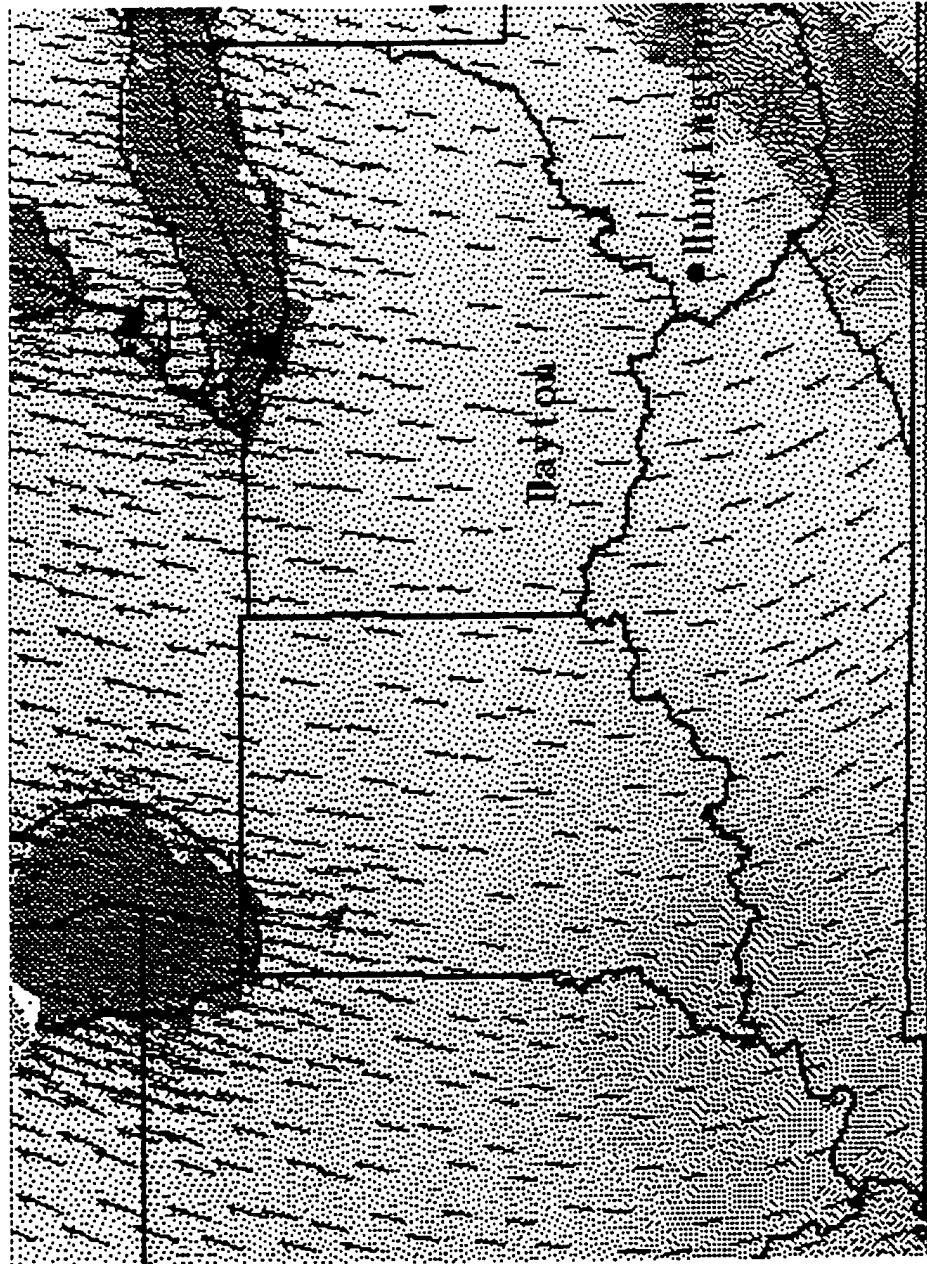
Appendix C: National Weather Service Maps and OMEGA Generated Maps for
MRF Validation

09/16 00Z 850hPa Analysis

160200Z Severe Tstm otlk valid until 161200Z (SHOW REGION).

Svr Tstm Watch #WS904 valid until DC



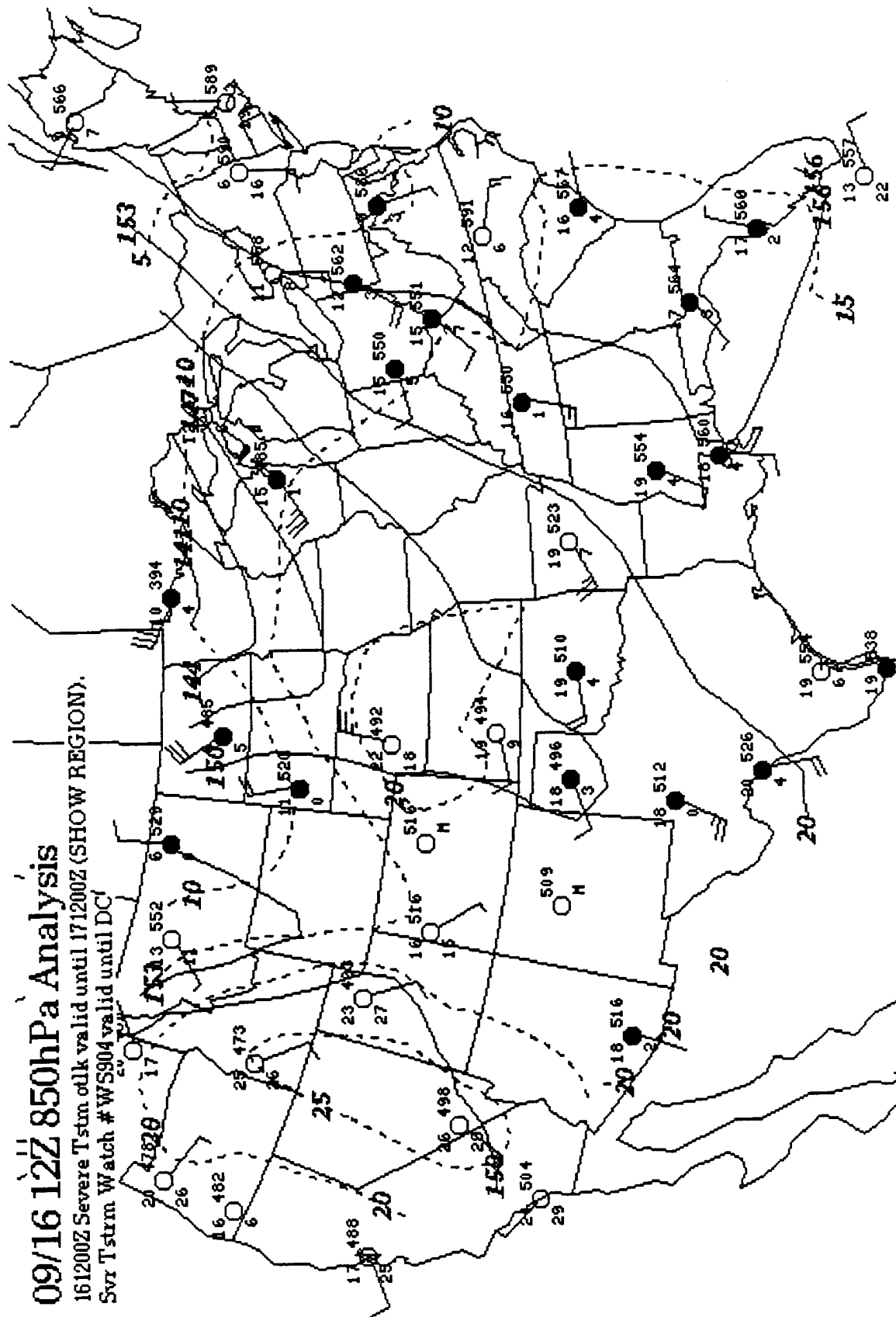


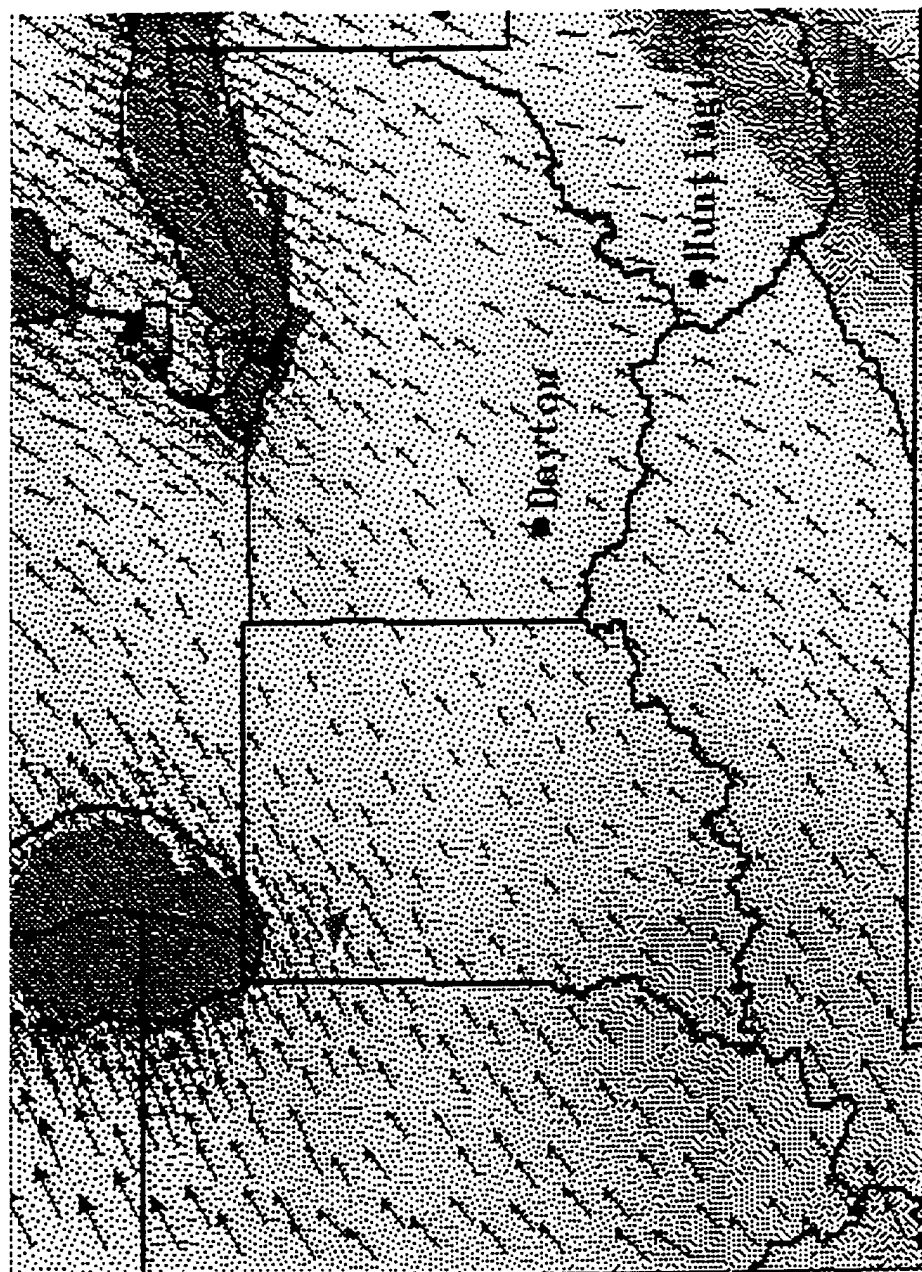
OMEGA Wind Field for 09/16 00Z 850 mb

09/16 12Z 850hPa Analysis
 161200Z Severe Tstm otlk valid until 171200Z (SHOW REGION).
 Svr Tstm Watch #WS904 valid until DCI

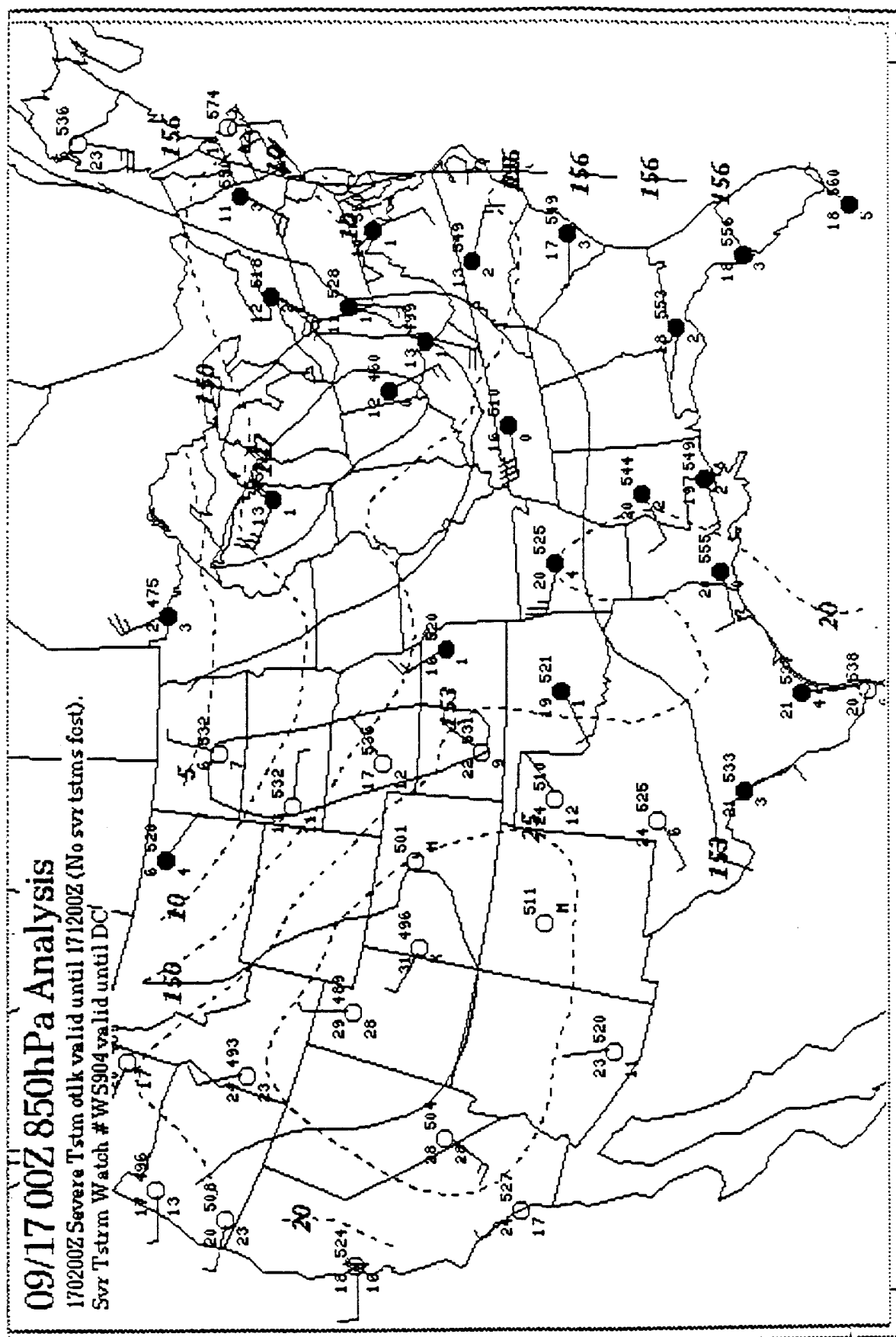
Sys Tstrm Watch #WS904 valid until DCI'

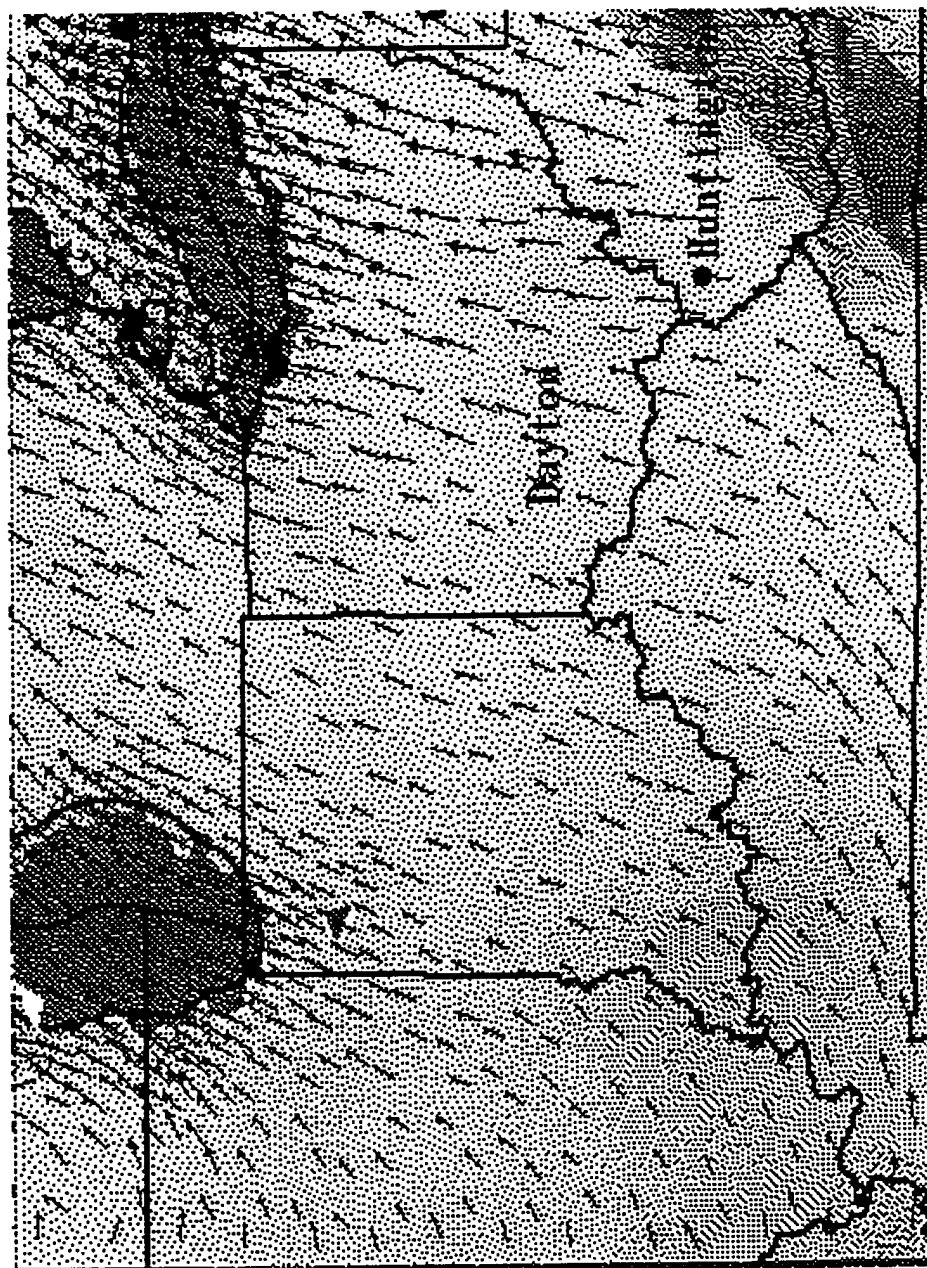
Sys Tstrm Watch #WS904 valid until DCI'





OMEGA Wind Field for 09/16 12Z 850 mb



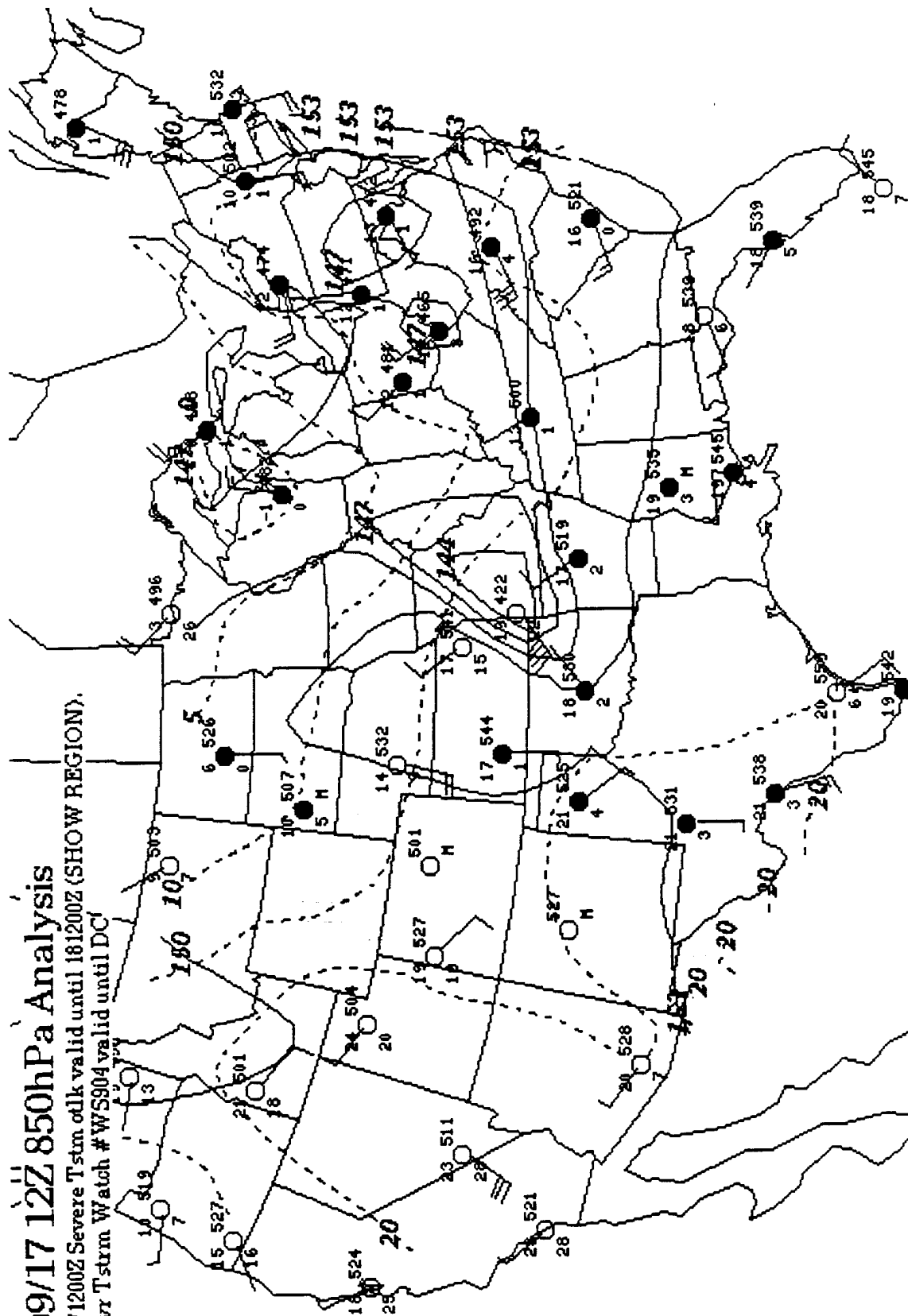


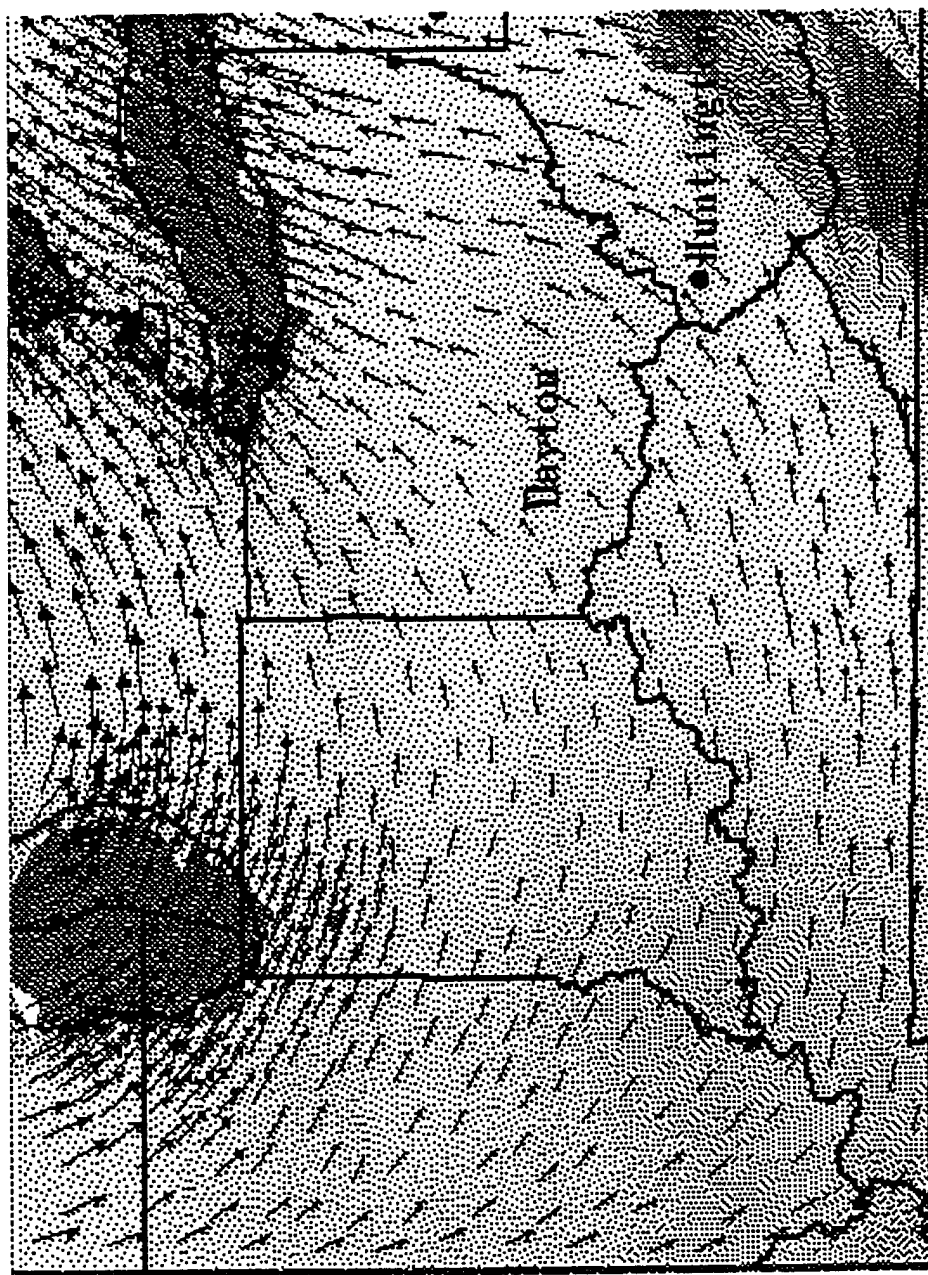
OMEGA Wind Field for 09/17 00Z 850 mb

09/17 12Z 850hPa Analysis

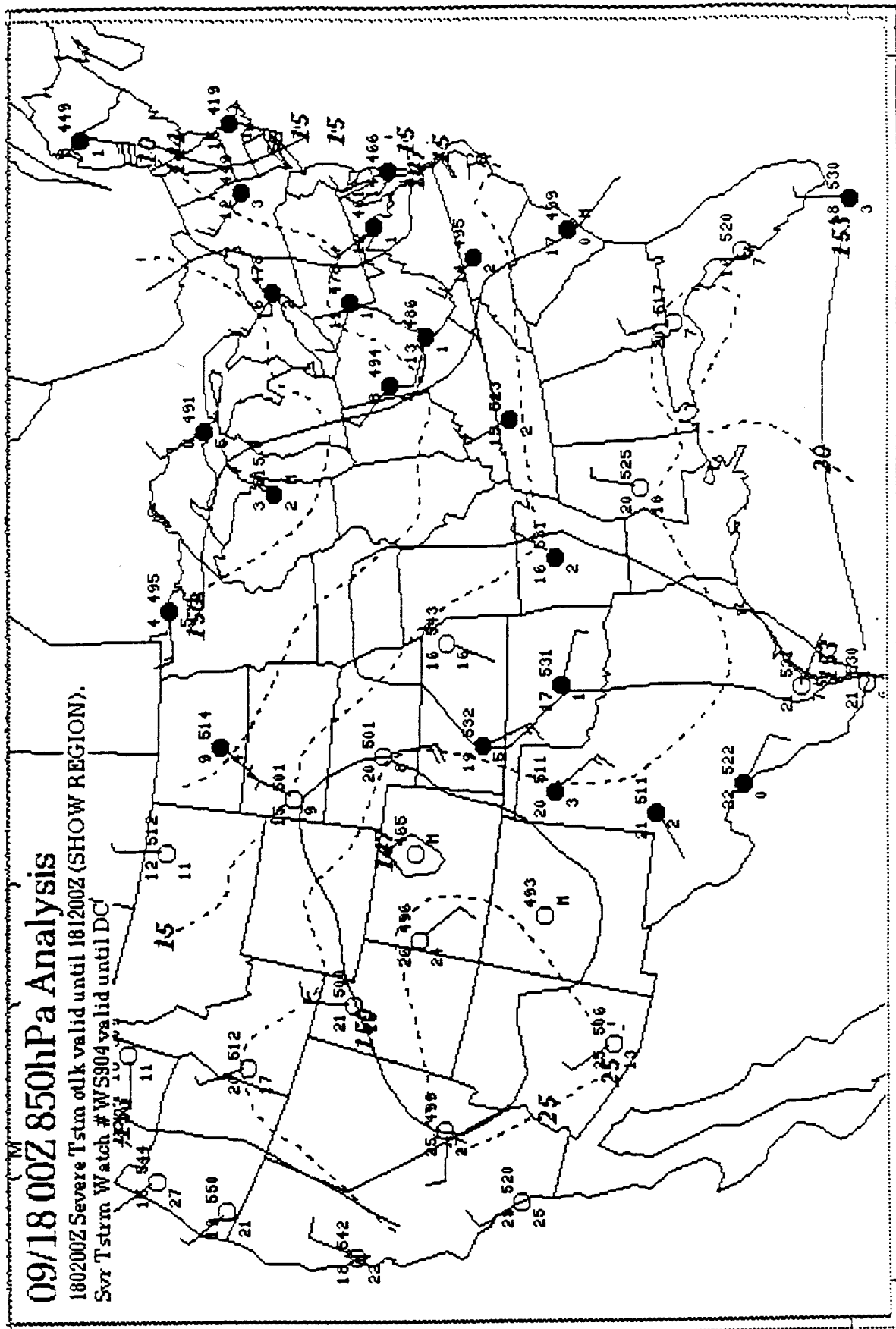
171200Z Severe Tstm otlk valid until 181200Z (SHOW REGION).

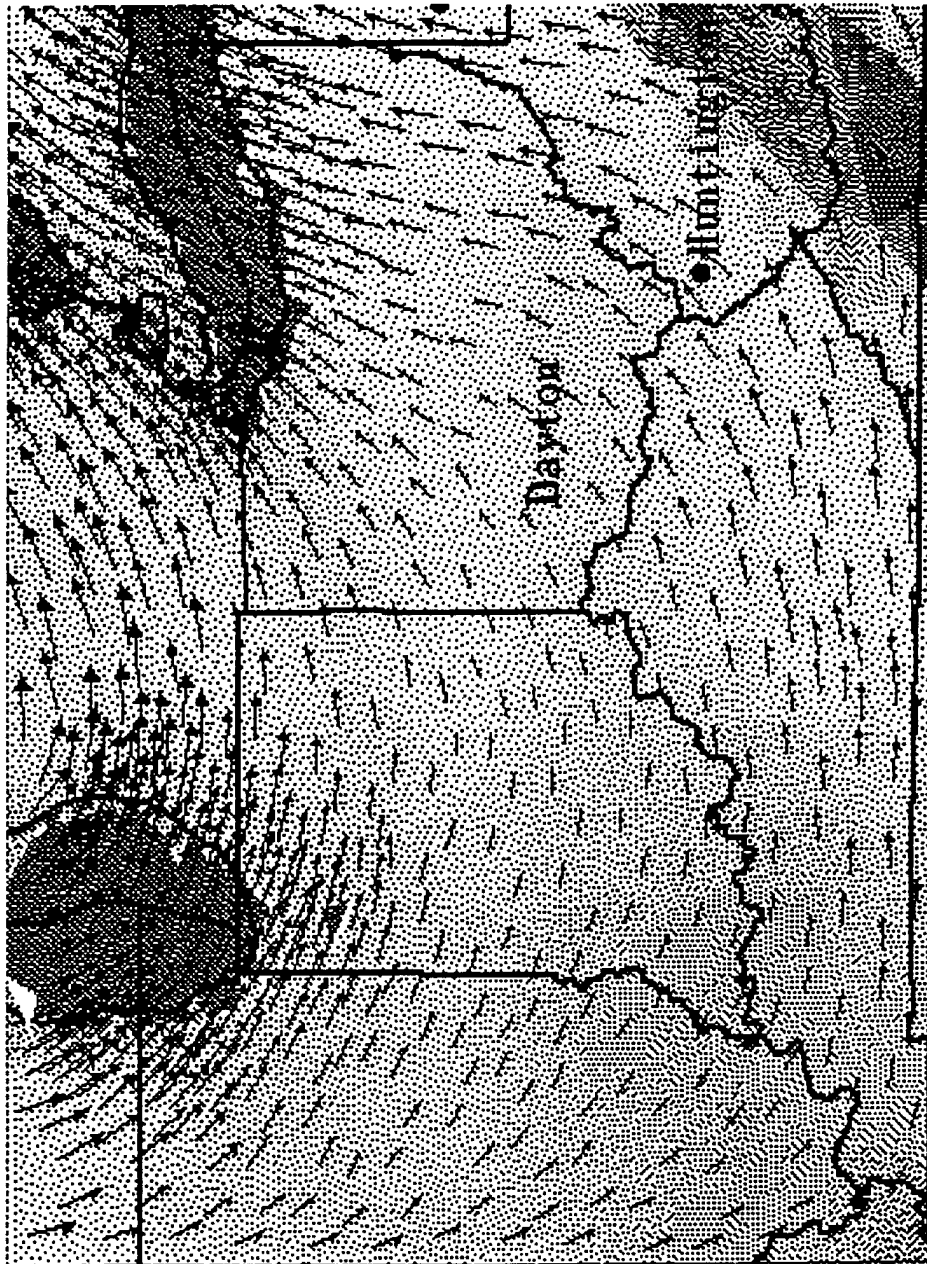
Svr Tstm Watch #WS904 valid until DC





OMEGA Wind Field for 09/17 12Z 850 mb



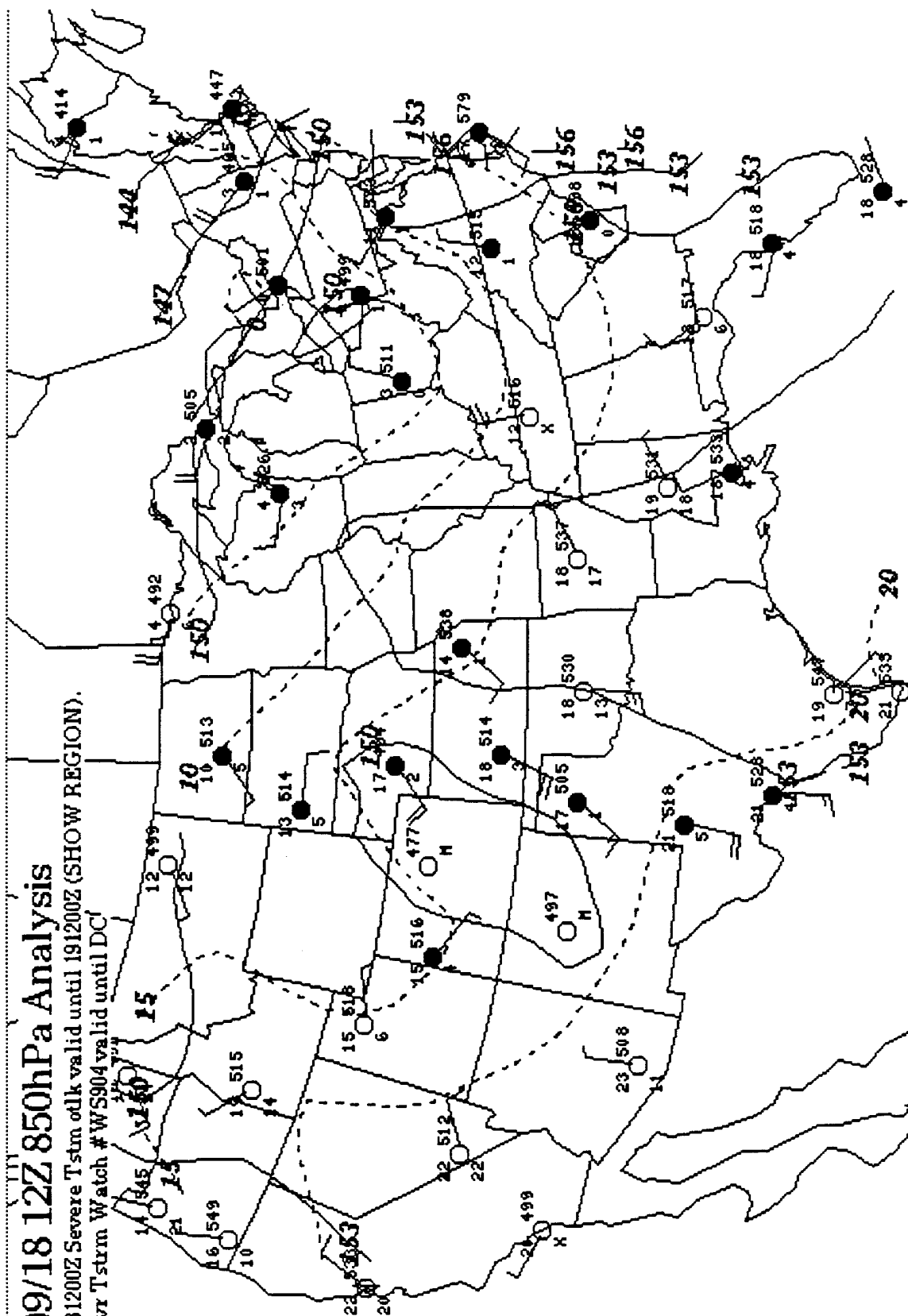


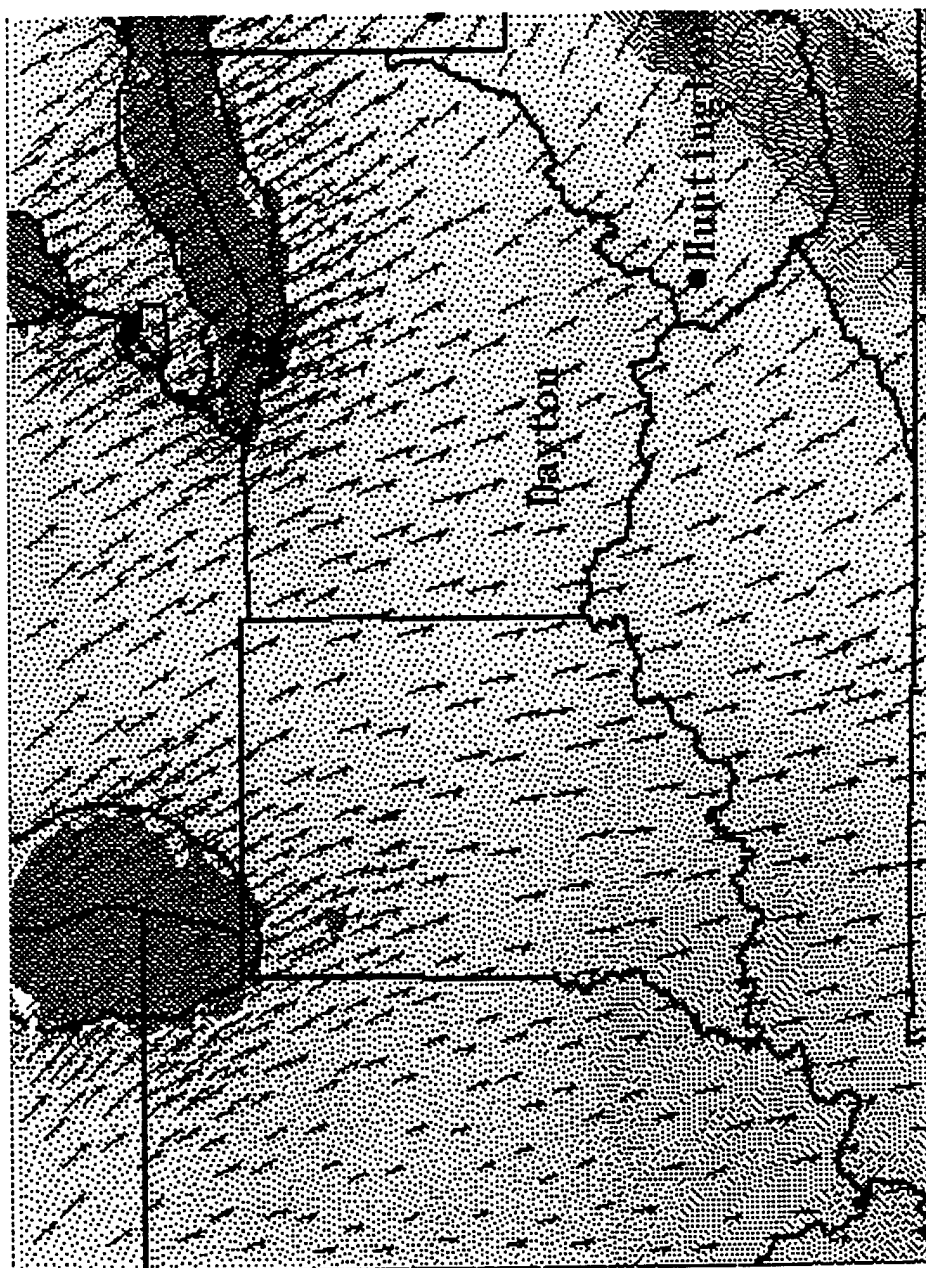
OMEGA Wind Field for 09/18 00Z 850 mb

09/18 12Z 850hPa Analysis

181200Z Severe Tstm otlk valid until 191200Z (SHOW REGION).

Svr Tstm Watch #WS904 valid until DC'



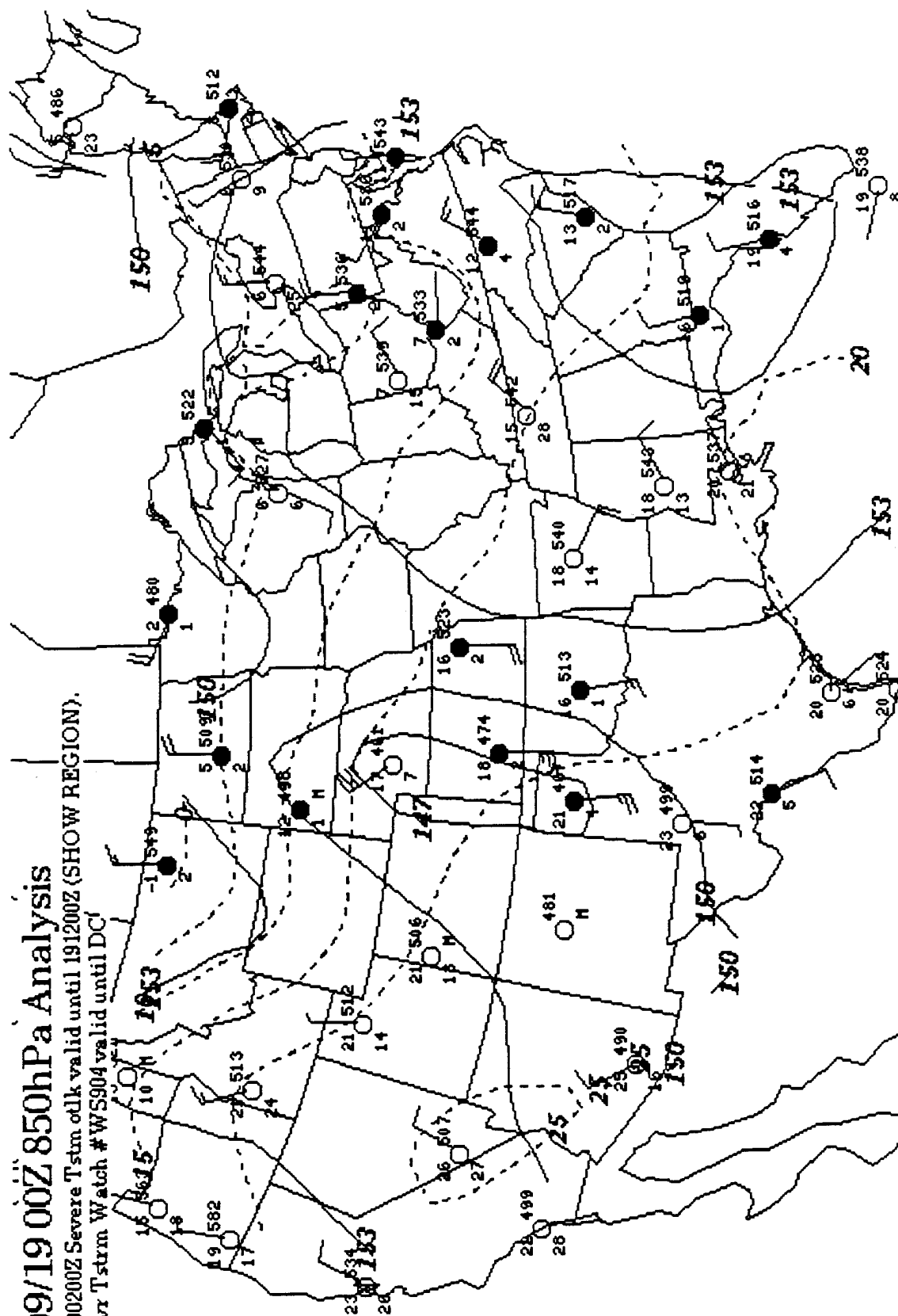


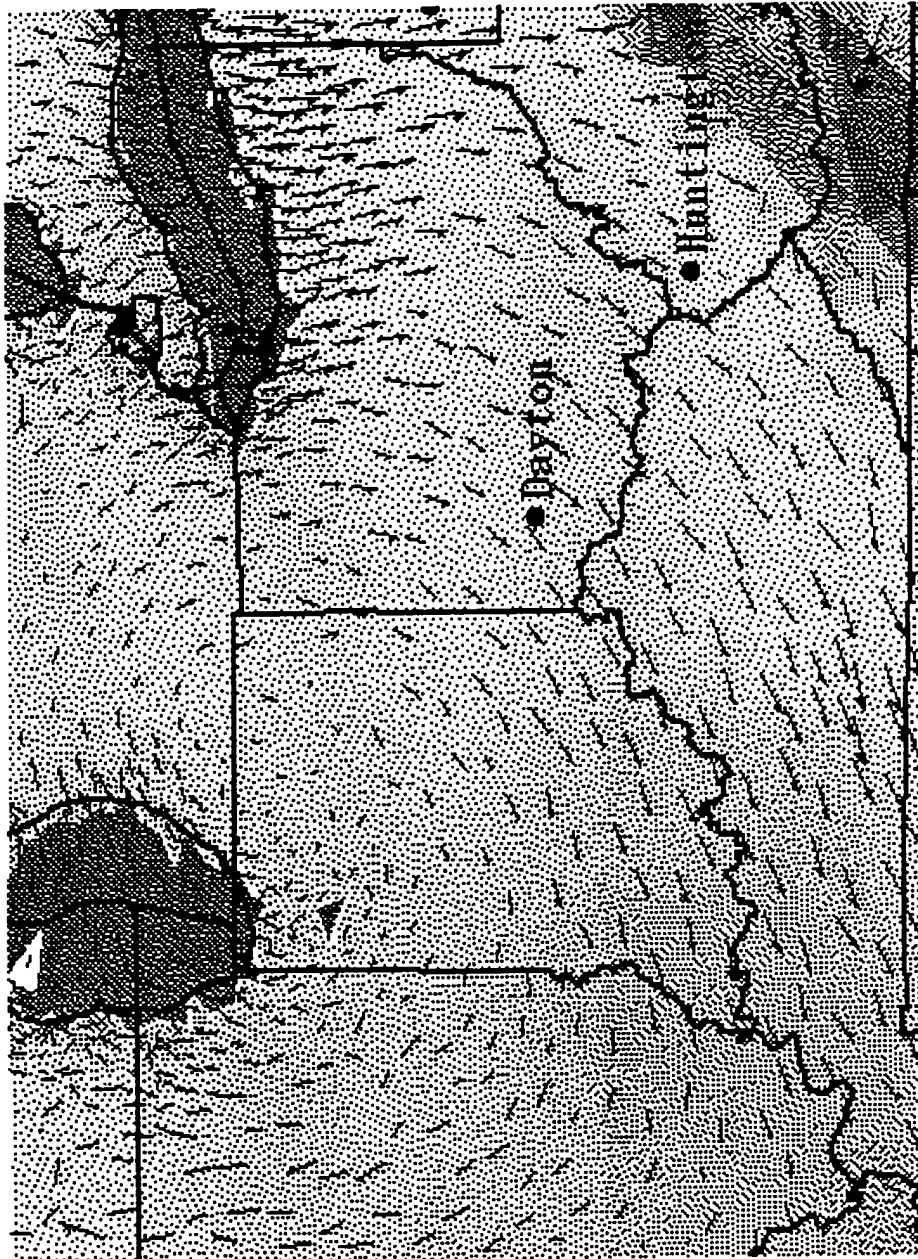
OMEGA Wind Field for 09/18 12Z 850 mb

9/19 00Z 850hPa Analysis

0200Z Severe Tstm otk valid until 191200Z (SHOW REGION).
Tstrm Watch #WS904 valid until DC

Svr Tstrm Watch #WS904 valid until DCI'





OMEGA Wind Field for 09/19 00Z 850 mb

Appendix D: Sample Maps for Deposition Using HIRAS Data

Täglicher Wetterbericht

des Meteorologischen Dienstes der Deutschen Demokratischen Republik

Herausgeber: Meteorologischer Dienst der DDR, Zentrale Wetterdienststelle

1500 Potsdam, Michendorfer Chaussee 23

Fernruf-Sammelnummer 3160, Telex-Nr. 015532

ISSN 0232-5573

Index 30086

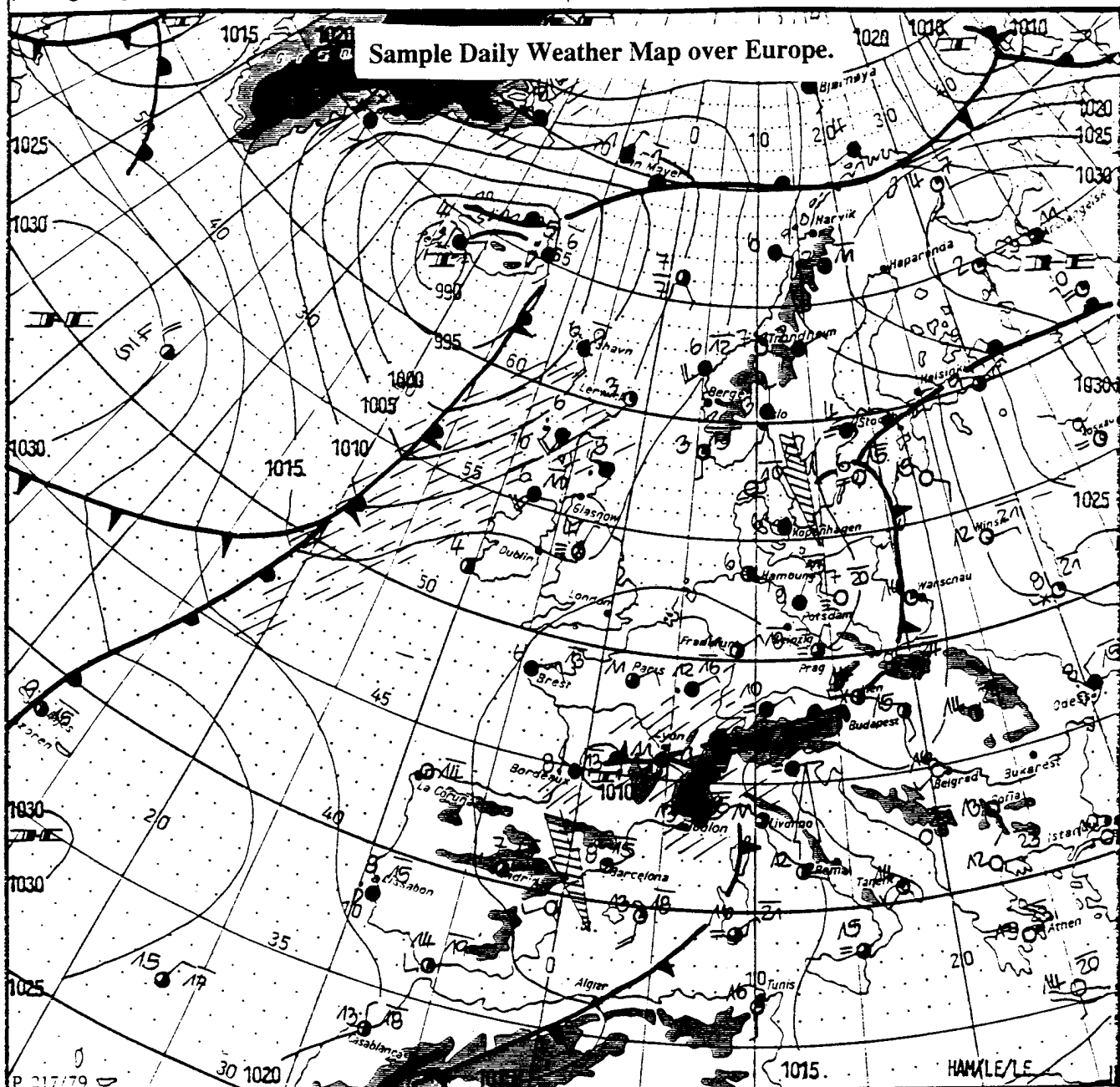
Nachdruck, auch auszugsweise, nur mit Quellenangabe gestattet.
Bezugspreis (monatlich 4,- M (einschließlich Beilagen) EVP 0,15 M.

AN EDV 403500

Jahrgang 40

Sonnabend, den 26. April 1986

Nr. 115



Wetterlage

26. 04. 86, 01h

M 1 : 30 000 000

	Warmfront		Stromung in Warmluft		Sprunregen		Graupelschauer		windstill		vulkanisch
	Kaltfront		Stromung in Kaltluft		feuchter Dunst		Hagelschauer		umlaufender Wind		heiter
	Okklusion		Niederschlagsgebiet		Reicher Nebel		Regenschauer		Nordost 5 km/h		wolkenig
	Konvergenzlinie		10°C Wassertemperatur		Schnee		Schneeschauer		Ost 10 km/h		stark bewölkt
	Hochdruckgebiet		15°C Wassertemperatur		Schneetreiben		Witterleuchten		Südost 10 km/h		bedeckt
	Hochdruckkeil		Tagesmaximum der Lufttemperatur des Vortages		Schneetreiben bzw. Sandsturm		Gewitter		Südwest 100 km/h		bedeckt nicht angebar
	Zwischenhoch		Nebel in der Umgebung		während der letzten Stunden, aber nicht zum Beobachtungsstunde 23.00						
	Tiefdruckgebiet										
	Tiefdruckkeil										
	Tiefdruckkeil										

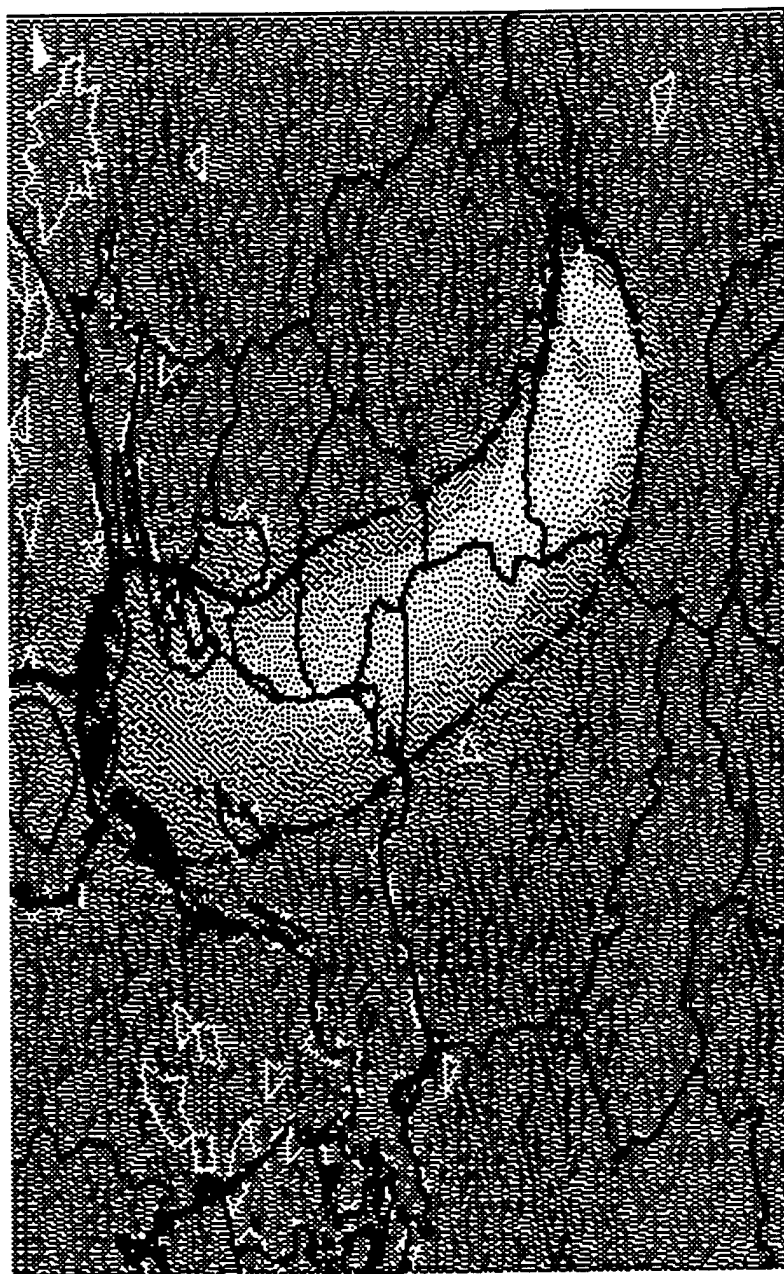
Erscheint täglich, nur im Postbezug erhältlich.
Bestellungen, Abbestellungen und Reklamationen sind
an den zuständigen Postzeitungsvertriebe zu richten

D.1

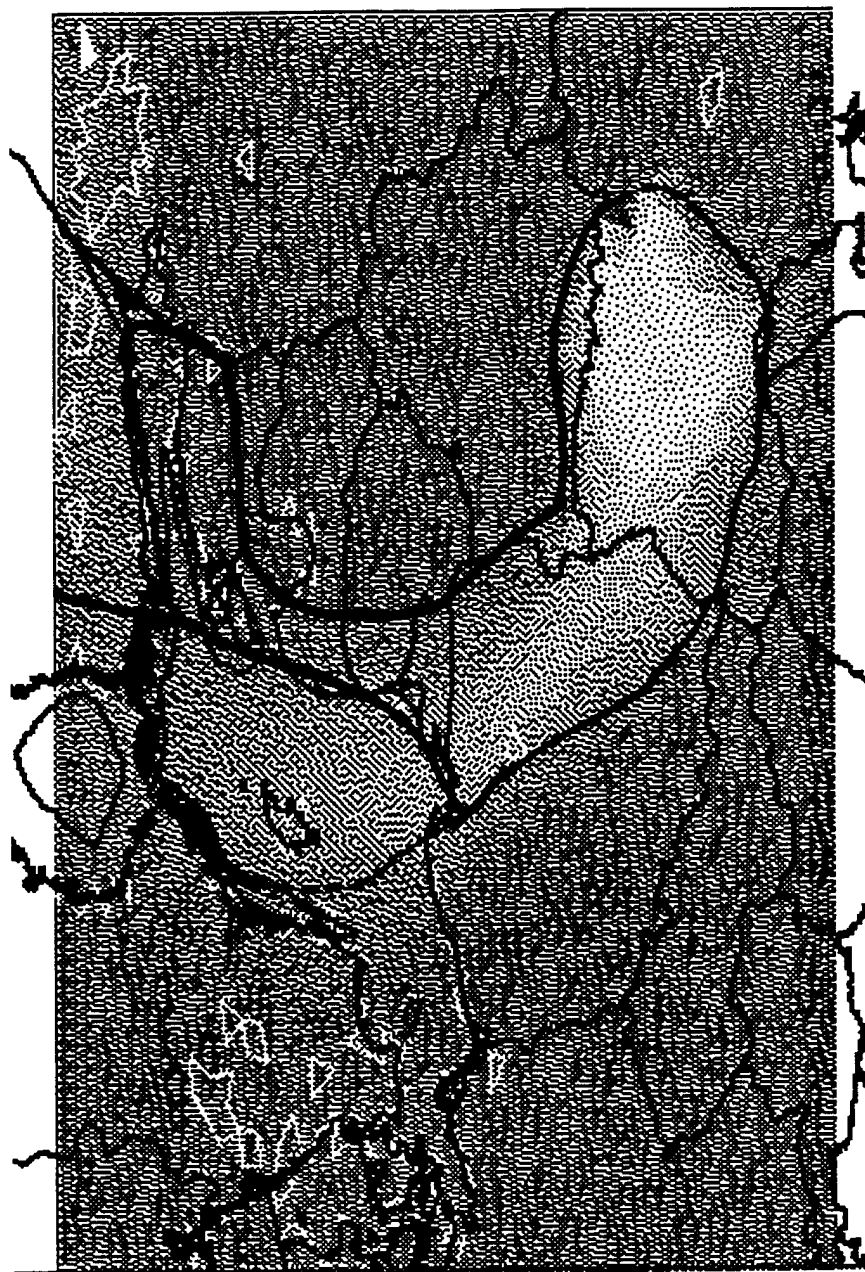
Alle Zeitangaben in MEZ
(Mitteleuropäische Zeit)



OMEGA Generated Footprint for Eulerian Tracer at 1500 meters, 04/27/86 00Z.



OMEGA Generated Footprint for Eulerian Tracer at 1500 meters, 04/27/86 12Z.



OMEGA Generated Concentration at 300 mb for Eulerian Tracer at 1500 meters,
04/28/86 00Z.

Appendix E: Chernobyl Source Term Defined by Fortran 90 Code

c Subroutine Chernobyl to model nuclear accident on 26 April 1986,
 c 0000Z. Source term is modeled according to the Technical
 c Specifications Document in "Evaluation of Long Range Atmospheric
 c Transport Models using Environmental Radioactivity Data From the
 c Chernobyl Accident", the ATMES Report.

c

```

    program chernobyl
    parameter(numsrc=12)
    integer i, maxid, iprt_id0(numsrc)
    real timeinj, prt_tim(numsrc+1), prt_mass(numsrc), prt_d0(numsrc),
& prt_lon0(numsrc), prt_lat0(numsrc), prt_alt0(numsrc),
& prt_rhd0(numsrc), prt_vap0(numsrc), prt_sx0(numsrc),
& prt_sy0(numsrc), prt_sz0(numsrc), fact
    character*6 modeadm

```

```

    fact = 4.5E+07*2.29E-25
    timeinj = 3600.
    modeadm = 'tracer'

```

```

    prt_tim(1) = 86400.
    prt_tim(2) = 86400+6.*60.*60.
    prt_mass(1) = 2.2E+16*fact*.2/6.
    prt_mass(2) = 2.2E+16*fact*.8/18.
    prt_mass(3) = 7.0E+15*fact/24.
    prt_mass(4) = 5.51E+15*fact/24.
    prt_mass(5) = 4.11E+15*fact/24.
    prt_mass(6) = 3.01E+15*fact/24.
    prt_mass(7) = prt_mass(6)
    prt_mass(8) = prt_mass(4)
    prt_mass(9) = 6.31E+15*fact/24.
    prt_mass(10) = 8.11E+15*fact/24.
    prt_mass(11) = 8.91E+15*fact/24.
    prt_mass(12) = 1.11E+14*fact/24.
    prt_alt0(1) = 1500.

```

```

    do i=1, numsrc

```

```

        prt_d0(i)=1.e-20
        iprt_id0(i)=i
        prt_lon0(i) = 30.15
        prt_lat0(i) = 51.17
        prt_rhd0(i)=1.e-20
        prt_vap0(i)=1.e-20
        prt_sx0(i)=400.
        prt_sy0(i)=400.
    end do

```

```
prt_sz0(i)=400.
```

c Now set altitude, each variation.

```
if (i .gt. 1 .and. i .lt. 4) prt_alt0(i) = 600.  
if (i .gt. 3) prt_alt0(i) = 300.
```

c Set time of release, each variation.

```
if (i .gt. 2) prt_tim(i) = (i-1)*86400.  
enddo
```

```
prt_tim(13) = prt_tim(12)+86400.
```

c Now let's write the output to a file

```
open(unit=1, file='case.adm', status='unknown')  
write (1, *) maxid  
write (1, *) numsrc  
write (1,100) timeinj  
100 format(f6.0)  
write (1, 110) modeadm  
110 format(a6)  
do i=1, numsrc  
write (1, 120) ipt_id0(i), prt_lon0(i), prt_lat0(i), prt_alt0(i),  
& prt_tim(i), prt_tim(i+1), prt_d0(i), prt_mass(i), prt_rhd0(i),  
& prt_vap0(i), prt_sx0(i), prt_sy0(i), prt_sz0(i)  
120 format(i8,12e15.7)  
enddo  
stop  
end
```

Bibliography

1. Anspaugh, Lynn R., Robert J. Catlin, and Marvin Goldman. "The Global Impact of the Chernobyl Reactor Accident," Science, 242: 1513-1517 (Dec 1988).
2. Bowers, James F., Elford G. Astling, and G.C. Dodd. "Atmospheric Transport and Dispersion Model Hierarchy," LPN-USATECOM-7-CO-R89-DPO-013, November 1989.
3. Carrascal, M.D., M. Puigcerver, and P. Puig. "Sensitivity of Gaussian Plume Model to Dispersion Specifications," Theoretical and Applied Climatology, 48: 147, 157 (1993).
4. Ciolek, John T. "Results of an Emergency Response Atmospheric Dispersion Model Comparison Using a State Accepted Statistical Protocol," American Meteorological Society, 1: 237-238 (Jan 1994).
5. Department of the Air Force. HIRAS USAFETAC Climatic Database Users Handbook No. 5. Asheville, N.C.: USAFETAC, 19 February 1991.
6. Desiato, F. "A Long-Range Dispersion Model Evaluation Study With Chernobyl Data," Atmospheric Environment, 26A: 2805-2820 (1992).
7. Fast, Jerome D. and B. Lance O'Steen. "Atmospheric and Dispersion Modeling in Areas of Highly Complex Terrain Employing a Four-Dimensional Data Assimilation Technique," American Meteorological Society, 1: 310-311 (Jan 1994).
8. Galmarini, S., G. Graziani, and C. Tassone. "The Atmospheric Long Range Transport Model LORAN and its Application to Chernobyl Release," Environmental Software, 7: 143-154 (1992).
9. Hanna, S.R. "Uncertainties in Air Quality Model Prediction," Boundary-layer Meteorology, 62:1-4. 3 (January 1993).
10. Heffter, Jerome L., and Gilbert J. Ferber. "Development and Verification of the Air Regional-Continental Transport and Dispersion Model," American Meteorological Society: 400-407 (1990).
11. Hummel, J.R., M.G. Cheifetz, and E.P. Shettle. "Development of Models for the Transport of Atmospheric Aerosols and Their Optical/IR Properties," American Meteorological Society. 421-426 (1990).

12. Ishikawa, H. "Development of Worldwide Version of System for Prediction of Environmental Emergency Dose Information: WSPEEDI. III.," Journal of Nuclear Science and Technology, 31: 969-978 (September 1994).
13. Izrael, Yu. A. et al. "Global and Regional Radioactive Contamination of the Former European USSR with Cesium-137," AFMIC-HT-023-094, November 1994.
14. Jagger, John. The Nuclear Lion. New York: Plenum Publishing Corporation, 1991.
15. Kaplan, Hadassah, et al. Transport and Diffusion in Turbulent Fields. The Netherlands: Kluwer Academic Publishers, 1993.
16. Klug, W. et al. Evaluation of Long Range Atmospheric Transport Models Using Environmental Radioactivity Data From the Chernobyl Accident: The ATMES Report. New York: Elsevier Applied Science, 1992.
17. Lieman and Alpert. "Investigation of the Planetary Boundary Layer Height Variations over Complex Terrain," Boundary-layer Meteorology, 62:1-4. 129 (January 1993).
18. Moran, M.D. and Roger .A. Pielke. "Delayed Shear Enhancement in Mesoscale Atmospheric Dispersion," American Meteorological Society, 1: 96 (Jan 1994).
19. Mullen, J.B., M.W. Chan, and I.H. Tombach. "Development and Validation of a Model for Diffusion in Complex Terrain," American Meteorological Society. 188-191 (1978).
20. Orlanski, I. "A Simple Boundary Condition for Unbounded Hyperbolic Flows," Journal of Computer Physics, 21: 251-269 (1976).
21. Pieldelievre, Jean Philippe, Luc Musson-Genon, and Francois Bompay. "MEDIA-- An Eulerian Model of Atmospheric Dispersion: First Validation on the Chernobyl Release," Journal of Applied Meteorology, 29: 1205-1220 (December 1990).
22. Pudykiewicz, Janusz. "A Predictive Atmospheric Tracer Model," Journal of the Meteorological Society of Japan, 68: 213-225 (April 1990).
23. Pudykiewicz, Janusz. "Simulation of the Chernobyl Dispersion With a 3-D Hemispheric Tracer Model," Tellus. Series B, Chemical and Physical Meteorology, 41B: 391-412 (September 1989).
24. Rantalainen, L. "The Importance of Mesoscale Phenomena on the Dispersion of Pollutants in the Vicinity of a Point-source Emission," Boundary-layer Meteorology, 62:1-4. 143 (January 1993).

25. Sherman, Christine A. "A Mass-Consistent Model for Wind Fields over Complex Terrain," Journal of Applied Meteorology, 17: 312-319 (March 1978).
26. Smith, F.B. and M.J. Clark. "The Transport and Deposition of Airborne Debris from the Chernobyl Nuclear Power Plant Accident With Special Emphasis on the Consequences to the United Kingdom," Great Britain Meteorological Office: 42: 6-13 (1989).
27. Täglicher Wetterbericht, 115-118: 1-4 (April 1986).
28. Taguchi, Shoichi. "Interhemispheric Exchange in the Troposphere by an Atmospheric Transport Model Based on Observed Winds," Meteorological Society of Japan, 71: 123-135 (February 1993).
29. Turner, D. Bruce. "Atmospheric Dispersion Modeling--A Critical Review," Journal of the Air Pollution Control Association, 29: 502-519 (May 1979).
30. Turner, D. Bruce. Workbook of Atmospheric Dispersion Estimates: An Introduction to Dispersion Modeling. Boca Raton: CRC Press, 1994.
31. Uliasz, Marek, Roger A. Stocker, and Roger A. Pielke. "Lagrangian Particle Modeling of Air Pollution Transport in Southwestern U.S.," American Meteorological Society, 1: 104 (Jan 1994).
32. Weil, J.C. "Evaluating Plume Dispersion Models: Expanding the Practice to Include the Model Physics," American Meteorological Society, 1: 224 (Jan 1994).

Vita

Captain Gordon R. Taylor was born at Wright-Patterson Air Force Base, Ohio, January 2, 1970. He graduated from Wells High School, Wells, Maine, in 1987. He received an Air Force Reserve Officer Training Corps scholarship to attend Clemson University in Clemson, South Carolina, where he received a Bachelor of Science Degree in Mechanical Engineering in 1991.

Captain Taylor earned a reserve commission as a second lieutenant in May 1991. He entered active duty in September 1991 and served as a contract programmer at Moody Air Force Base, Georgia until May 1994. He attended the Air Force Institute of Technology from May 1994 to December 1995 and graduated with a Masters of Science Degree in Engineering and Environmental Management in December 1995. He was then stationed at Minot Air Force Base, North Dakota.

Permanent Address:

Gordon Taylor
123 Westwood Drive
Belton, SC 29627

REPORT DOCUMENTATION PAGE			Form Approved OMB No. 0704-0188	
Public reporting burden for this collection of information is estimated to average 1 hour per response, including the time for reviewing instructions, searching existing data sources, gathering and maintaining the data needed, and completing and reviewing the collection of information. Send comments regarding this burden estimate or any other aspect of this collection of information, including suggestions for reducing this burden, to Washington Headquarters Services, Directorate for Information Operations and Reports, 1215 Jefferson Davis Highway, Suite 1204, Arlington, VA 22202-4302, and to the Office of Management and Budget, Paperwork Reduction Project (0704-0188), Washington, DC 20503.				
1. AGENCY USE ONLY (Leave blank)		2. REPORT DATE DEC 95		3. REPORT TYPE AND DATES COVERED Preliminary (Mar 95 - Dec 95)
4. TITLE AND SUBTITLE VALIDATION OF OPERATIONAL MULTISCALE ENVIRONMENT MODEL WITH GRID ADAPTIVITY (OMEGA)			5. FUNDING NUMBERS	
6. AUTHOR(S) Gordon R. Taylor				
7. PERFORMING ORGANIZATION NAME(S) AND ADDRESS(ES) AIR FORCE INSTITUTE OF TECHNOLOGY AFIT/ENP 2950 P STREET WRIGHT-PATTERSON AFB OH 45433-7400			8. PERFORMING ORGANIZATION REPORT NUMBER	
9. SPONSORING / MONITORING AGENCY NAME(S) AND ADDRESS(ES) <i>Lt Col James Hodge</i> DEFENSE NUCLEAR AGENCY 6801 TELEGRAPH ROAD ALEXANDRIA, VA 22310-3398			10. SPONSORING / MONITORING AGENCY REPORT NUMBER	
11. SUPPLEMENTARY NOTES				
12a. DISTRIBUTION / AVAILABILITY STATEMENT Approved for public release; distribution unlimited			12b. DISTRIBUTION CODE	
13. ABSTRACT (Maximum 200 words) The Defense Nuclear Agency (DNA) is improving the military's capability to forecast dosage and hazard levels due to release of chemical, biological, and nuclear agents. During Operation DESERT STORM the military realized the need for models to predict risk levels for military personnel assigned proximate to missile attacks. One project associated with this is the continuing development of the Operational Multiscale Environmental Model with Grid Adaptivity (OMEGA). DNA has sponsored AFIT to validate OMEGA with focus on incorporating weather data obtained from Air Force Combat Climatology Center for the period of the Chernobyl Nuclear Accident. The physics of the model is tested using National Weather Service Medium Range Forecast data by comparing predicted wind fields for three weather stations with analysis maps. The model is further tested using the data generated at Air Force Combat Climatology Center for the first three days following the release at the Chernobyl Nuclear Plant. A user-defined source term was developed to simulate the release of radionuclides from the plant. Analysis from paired t-tests shows statistically how well OMEGA predicts wind fields. The results show qualitatively the promise of OMEGA to meet the needs of the Defense Nuclear Agency as the model is under development.				
14. SUBJECT TERMS Atmosphere models			15. NUMBER OF PAGES 97	
			16. PRICE CODE	
17. SECURITY CLASSIFICATION OF REPORT UNCLASSIFIED	18. SECURITY CLASSIFICATION OF THIS PAGE UNCLASSIFIED	19. SECURITY CLASSIFICATION OF ABSTRACT UNCLASSIFIED	20. LIMITATION OF ABSTRACT SAR	